

**REPORT ON A HELICOPTER-BORNE
VERSATILE TIME DOMAIN ELECTROMAGNETIC (VTEM) AND
AEROMAGNETIC GEOPHYSICAL SURVEY**

Expo Block and Ellen Creek Block

Finlayson Lake, Yukon

For:

18526 Yukon Inc.

By:

Geotech Ltd.

245 Industrial Parkway North

Aurora, Ont., CANADA, L4G 4C4

Tel: 1.905.841.5004

Fax: 1.905.841.0611

www.geotech.ca

Email: info@geotech.ca

Survey flown during August 2014

Project GL140269

October, 2014

TABLE OF CONTENTS

Executive Summary	iii
1. INTRODUCTION	1
1.1 General Considerations	1
1.2 Survey and System Specifications	2
1.3 Topographic Relief and Cultural Features	3
2. DATA ACQUISITION	5
2.1 Survey Area	5
2.2 Survey Operations	5
2.3 Flight Specifications	6
2.4 Aircraft and Equipment	6
2.4.1 Survey Aircraft	6
2.4.2 Electromagnetic System	6
2.4.3 Airborne magnetometer	10
2.4.4 Radar Altimeter	10
2.4.5 GPS Navigation System	10
2.4.6 Digital Acquisition System	10
2.5 Base Station	11
3. PERSONNEL	12
4. DATA PROCESSING AND PRESENTATION	13
4.1 Flight Path	13
4.2 Electromagnetic Data	13
4.3 Magnetic Data	14
5. DELIVERABLES	15
5.1 Survey Report	15
5.2 Maps	15
5.3 Digital Data	16
6. CONCLUSIONS AND RECOMMENDATIONS	19

LIST OF FIGURES

Figure 1: Property Location	1
Figure 2: Survey area location on Google Earth	2
Figure 3: Flight path over a Google Earth Image – Expo Block	3
Figure 4: Flight path over a Google Earth Image – Ellen Creek Block	4
Figure 5: VTEM Transmitter Current Waveform	6
Figure 6: VTEM System Configuration.	9
Figure 7: Image of time-constant (τ calculated from dBz/dt data) with contours of the calculated vertical magnetic gradient (CVG of TMI)	20

LIST OF TABLES

Table 1: Survey Specifications	5
Table 2: Survey schedule	5
Table 3: Off-Time Decay Sampling Scheme	7
Table 4: Acquisition Sampling Rates	10
Table 5: Geosoft GDB Data Format	16
Table 6: Geosoft Resistivity Depth Image GDB Data Format	17
Table 7: Geosoft database for the VTEM waveform	18

APPENDICES

A. Survey location maps	
B. Survey Block Coordinates.....	
C. Geophysical Maps	
D. Generalized Modelling Results of the VTEM System.....	
E. EM Time Constant (TAU) Analysis	
F. TEM Resistivity Depth Imaging (RDI).....	
G. Resistivity Depth Images (RDI)	

REPORT ON A HELICOPTER-BORNE VERSATILE TIME DOMAIN ELECTROMAGNETIC (VTEM) and AEROMAGNETIC SURVEY

Expo Block and Ellen Creek Block
Finlayson Lake, Yukon

Executive Summary

During August 21st to August 29th, 2014 Geotech Ltd. carried out a helicopter-borne geophysical survey over the Expo and Ellen Creek Blocks located near Finlayson Lake Yukon, Canada.

Principal geophysical sensors included a versatile time domain electromagnetic (VTEM) system, and a caesium magnetometer. Ancillary equipment included a GPS navigation system and a radar altimeter. A total of 579 line-kilometres of geophysical data were acquired.

In-field data quality assurance and preliminary processing were carried out on a daily basis during the acquisition phase. Preliminary and final data processing, including generation of final digital data and map products were undertaken from the office of Geotech Ltd. in Aurora, Ontario.

The processed survey results are presented as the following maps:

- Total Magnetic Intensity
- B-Field Z Component Channel grid
- Calculated Time Constant (TAU)
- Electromagnetic stacked profiles of the B-field Z component
- Electromagnetic stacked profiles of the dB/dt Z component

Digital data includes all electromagnetic and magnetic products, ancillary data and the VTEM waveform.

This survey report describes the procedures for data acquisition, processing, final image presentation and the specifications for the digital data set.

1. INTRODUCTION

1.1 General Considerations

Geotech Ltd. performed a helicopter-borne geophysical survey over the Expo and Ellen Creek Blocks located near Finlayson Lake, Yukon, Canada (Figure 1 & Figure 2).

Ron Berdahl represented 18526 Yukon Inc. during the data acquisition and data processing phases of this project.

The geophysical surveys consisted of helicopter borne EM using the versatile time-domain electromagnetic (VTEM) system with Z component measurements and aeromagnetics using a caesium magnetometer. A total of 579 line-km of geophysical data were acquired during the survey.

The crew was based out of Finlayson Lake for the acquisition phase of the survey. Survey flying started on August 21st, 2014 and was completed on August 29th, 2014.

Data quality control and quality assurance, and preliminary data processing were carried out on a daily basis during the acquisition phase of the project. Final data processing followed immediately after the end of the survey. Final reporting, data presentation and archiving were completed from the Aurora office of Geotech Ltd. in October, 2014.



Figure 1: Property Location.

1.2 Survey and System Specifications

The survey areas are located near Finlayson Lake in Yukon (Figure 2).

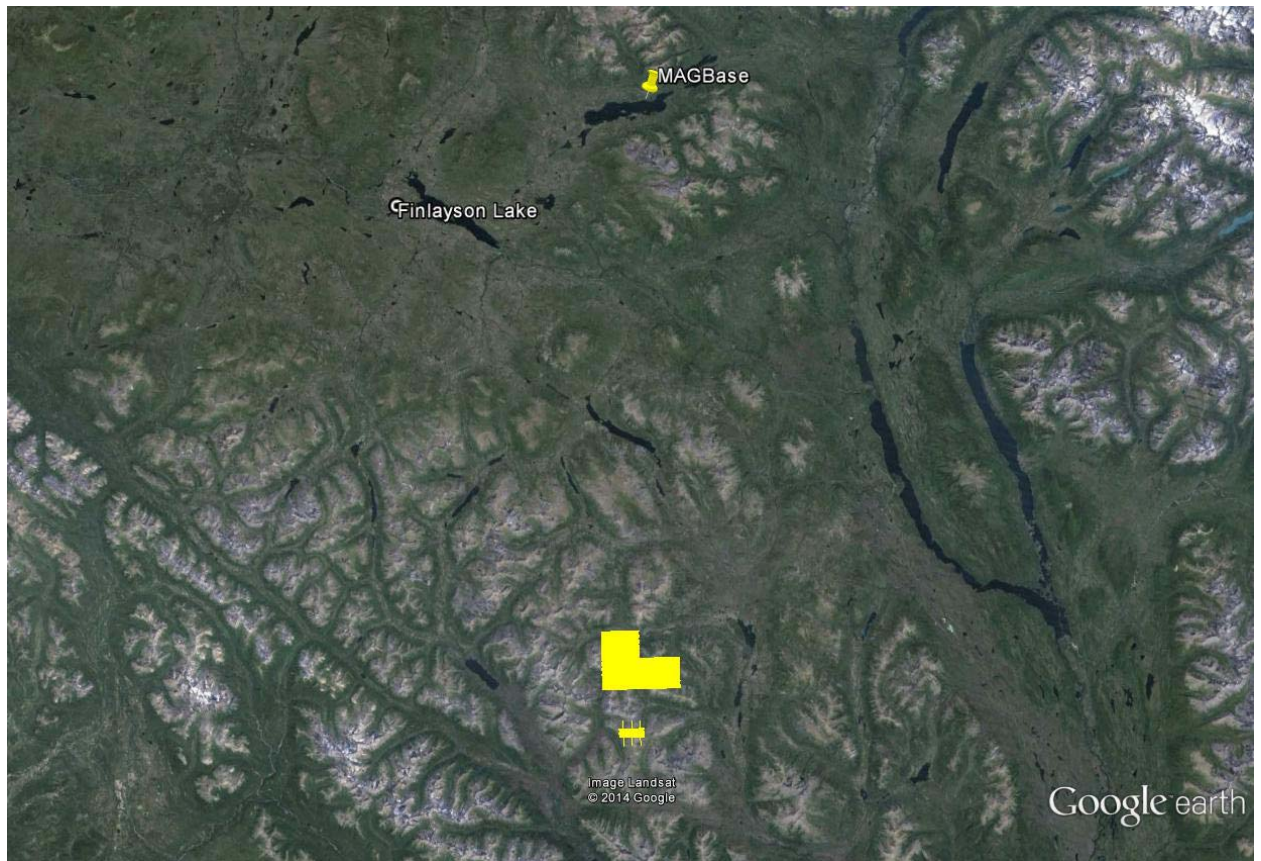


Figure 2: Survey area location on Google Earth.

Both areas were flown in an east to west ($N 90^{\circ} E$ azimuth) direction with traverse line spacing of 100 metres as depicted in Figures 3 to 4. Tie lines were flown perpendicular to the traverse lines at a spacing of 1000 metres ($N 0^{\circ} E$ azimuth).

For more detailed information on the flight spacing and direction see Table 1.

1.3 Topographic Relief and Cultural Features

Topographically, the survey areas exhibit a high relief with elevations ranging from 1158 to 1998 metres above mean sea level over an area of 53 square kilometres (Figure 3 to 4).

There are various rivers and streams running through the survey area which connect various lakes. There are no visible signs of culture such as roads or buildings throughout the survey area.

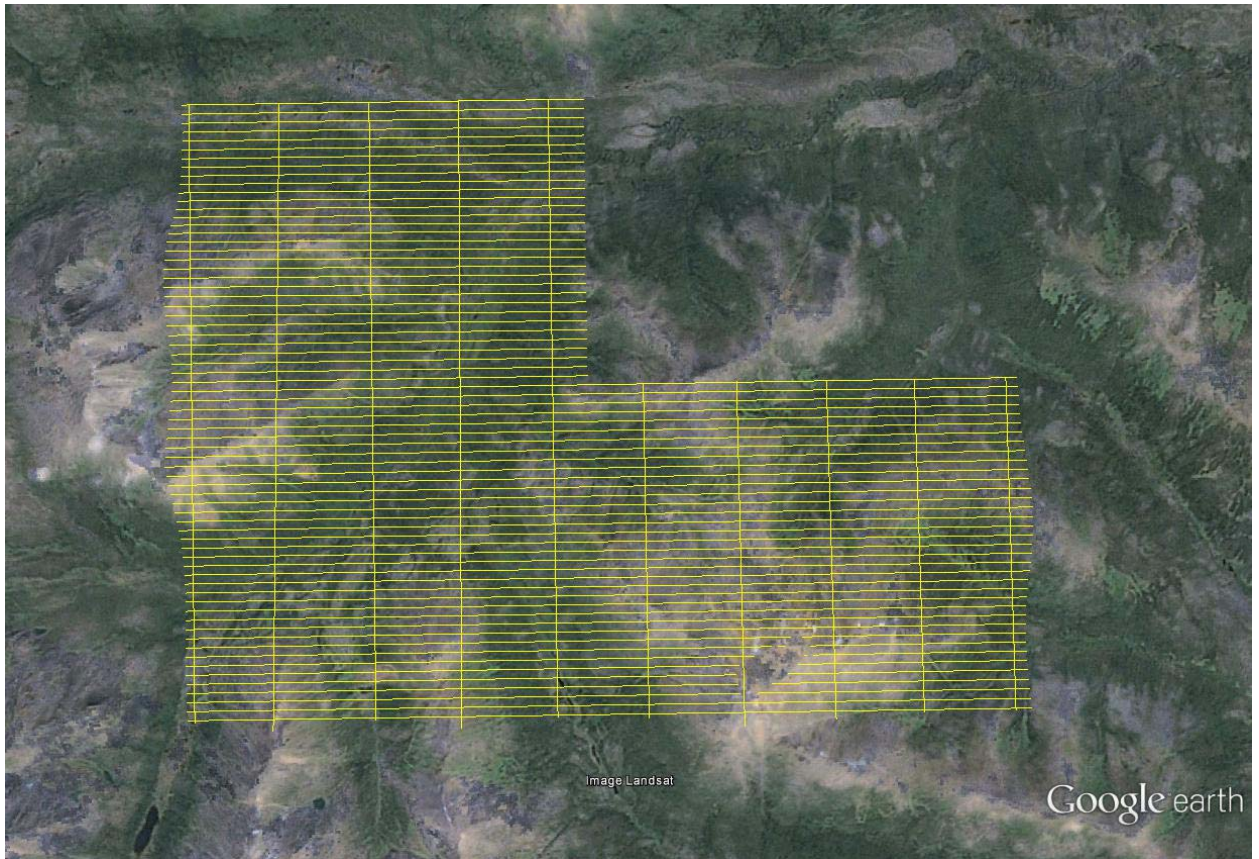


Figure 3: Flight path over a Google Earth Image – Expo Block

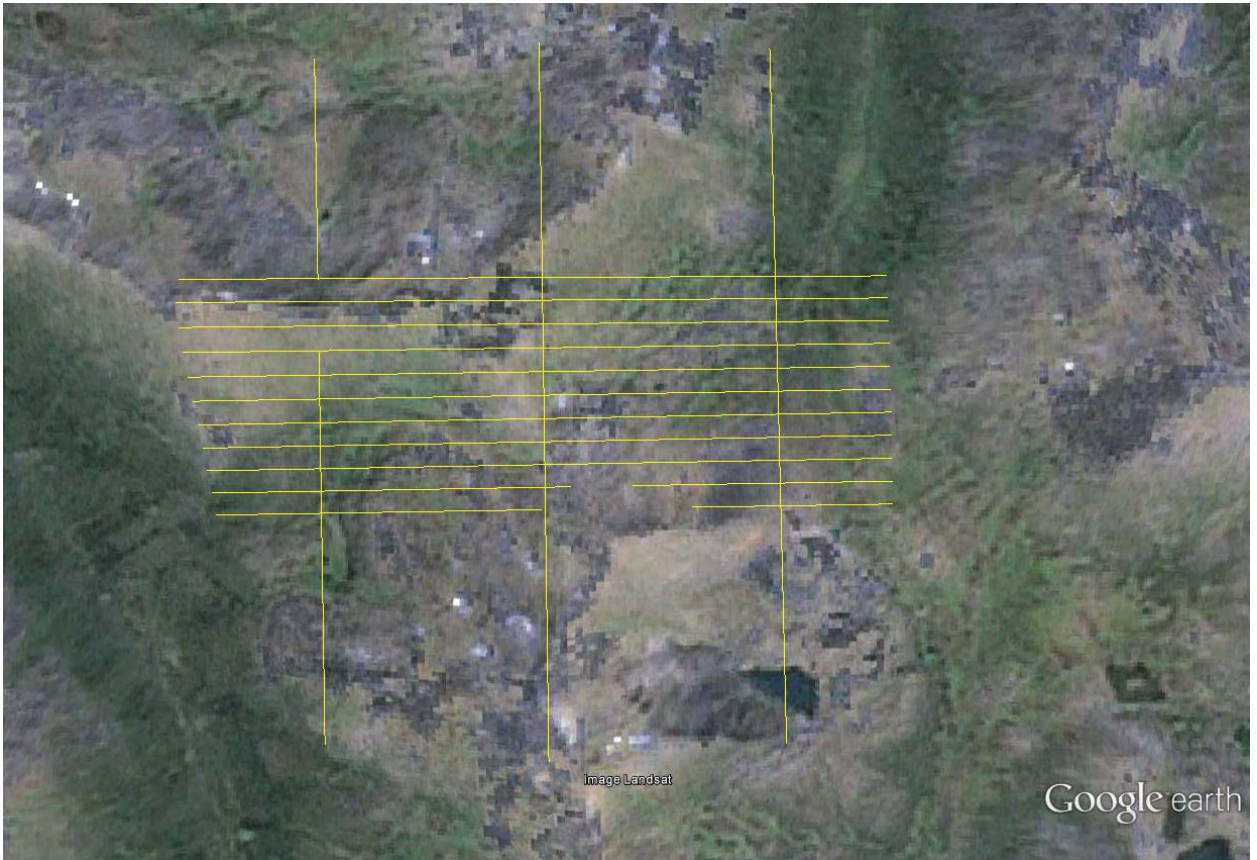


Figure 4: Flight path over a Google Earth Image – Ellen Creek Block

2. DATA ACQUISITION

2.1 Survey Area

The survey areas (see Figure 2 and Appendix A) and general flight specifications are as follows:

Table 1: Survey Specifications

Survey block	Line spacing (m)	Area (Km ²)	Planned ¹ Line-km	Actual Line-km	Flight direction	Line numbers
Expo	Traverse: 100	49	485	493	N 90° E / N 270° E	L1000 – L1680
	Tie: 1000		52	54	N 0° E / N 180° E	T2000 – T2090
Ellen Creek	Traverse: 100	4	33	34	N 90° E / N 270° E	L3000 – L3100
	Tie: 1000		9	9	N 0° E / N 180° E	T4000 – T4020
TOTAL		53	579	590		

Survey block boundaries co-ordinates are provided in Appendix B.

2.2 Survey Operations

Survey operations were based out of Finlayson Lake from August 2st to August 29^h, 2014. The following table shows the timing of the flying.

Table 2: Survey schedule

Date	Flight #	Flow km	Block	Crew location	Comments
21-Aug-2014				Finlayson Lake, Yukon	Mobilization
22-Aug-2014				Finlayson Lake, Yukon	Crew arrived
23-Aug-2014				Finlayson Lake, Yukon	System assembly
24-Aug-2014				Finlayson Lake, Yukon	System assembly & helicopter arrived
25-Aug-2014				Finlayson Lake, Yukon	Helicopter install & testing
26-Aug-2014	1,2	93		Finlayson Lake, Yukon	93 km flown limited due to weather
27-Aug-2014				Finlayson Lake, Yukon	No production due to weather & system tech
28-Aug-2014	3,4,5,6	459		Finlayson Lake, Yukon	459km flown
29-Aug-2014	7	27		Finlayson Lake, Yukon	Remaining kms were flown – flying complete

¹ Note: Actual Line kilometres represent the total line kilometres in the final database. These line-km normally exceed the Planned line-km, as indicated in the survey NAV files.

2.3 Flight Specifications

During the survey the helicopter was maintained at a mean altitude of 106 metres above the ground with an average survey speed of 80 km/hour. This allowed for an average EM transmitter-receiver loop terrain clearance of 70 metres and a magnetic sensor clearance of 93 metres.

The on board operator was responsible for monitoring the system integrity. He also maintained a detailed flight log during the survey, tracking the times of the flight as well as any unusual geophysical or topographic features.

On return of the aircrew to the base camp the survey data was transferred from a compact flash card (PCMCIA) to the data processing computer. The data were then uploaded via ftp to the Geotech office in Aurora for daily quality assurance and quality control by qualified personnel.

2.4 Aircraft and Equipment

2.4.1 Survey Aircraft

The survey was flown using a Eurocopter Aerospatiale (Astar) 350 B3 helicopter, registration C-GEOJ. The helicopter is owned and operated by Geotech Aviation. Installation of the geophysical and ancillary equipment was carried out by a Geotech Ltd crew.

2.4.2 Electromagnetic System

The electromagnetic system was a Geotech Time Domain EM (VTEM) system. VTEM, with the serial number 17 had been used for the survey. The configuration is as indicated in Figure 6

The VTEM Receiver and transmitter coils were in concentric-coplanar and Z-direction oriented configuration. The EM transmitter-receiver loop was towed at a mean distance of 35 metres below the aircraft as shown in Figure 6. The VTEM transmitter current waveform is shown diagrammatically in Figure 5.

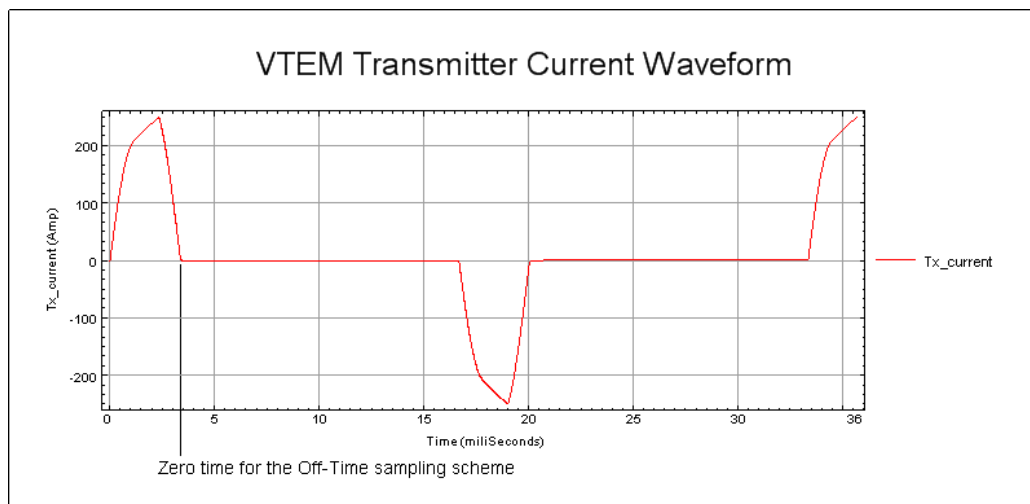


Figure 5: VTEM Transmitter Current Waveform

The VTEM decay sampling scheme is shown in Table 3 below. Thirty-five time measurement gates were used for the final data processing in the range from 0.096 to 10.667 msec. Zero time for the off-time sampling scheme is equal to the current pulse width and is defined as the time near the end of the turn-off ramp where the di/dt waveform falls to 1/2 of its peak value.

Table 3: Off-Time Decay Sampling Scheme

VTEM Decay Sampling Scheme				
Index	Start	End	Middle	Width
Milliseconds				
14	0.090	0.103	0.096	0.013
15	0.103	0.118	0.110	0.015
16	0.118	0.136	0.126	0.018
17	0.136	0.156	0.145	0.020
18	0.156	0.179	0.167	0.023
19	0.179	0.206	0.192	0.027
20	0.206	0.236	0.220	0.030
21	0.236	0.271	0.253	0.035
22	0.271	0.312	0.290	0.040
23	0.312	0.358	0.333	0.046
24	0.358	0.411	0.383	0.053
25	0.411	0.472	0.440	0.061
26	0.472	0.543	0.505	0.070
27	0.543	0.623	0.580	0.081
28	0.623	0.716	0.667	0.093
29	0.716	0.823	0.766	0.107
30	0.823	0.945	0.880	0.122
31	0.945	1.086	1.010	0.141
32	1.086	1.247	1.161	0.161
33	1.247	1.432	1.333	0.185
34	1.432	1.646	1.531	0.214
35	1.646	1.891	1.760	0.245
36	1.891	2.172	2.021	0.281
37	2.172	2.495	2.323	0.323
38	2.495	2.865	2.667	0.370
39	2.865	3.292	3.063	0.427
40	3.292	3.781	3.521	0.490
41	3.781	4.341	4.042	0.560
42	4.341	4.987	4.641	0.646
43	4.987	5.729	5.333	0.742
44	5.729	6.581	6.125	0.852
45	6.581	7.560	7.036	0.979
46	7.560	8.685	8.083	1.125

VTEM Decay Sampling Scheme				
Index	Start	End	Middle	Width
Milliseconds				
47	8.685	9.977	9.286	1.292
48	9.977	11.458	10.667	1.482

VTEM system specification:

Transmitter

- Transmitter loop diameter: 17.6 m
- Number of turns: 4
- Effective Transmitter loop area: 973 m²
- Transmitter base frequency: 30 Hz
- Peak current: 250 A
- Pulse width: 3.39 ms
- Wave form shape: Bi-polar trapezoid
- Peak dipole moment: 243,285 nIA
- Actual average EM transmitter-receiver loop terrain clearance: 70 metres above the ground

Receiver

- Z-Coil diameter: 1.2 m
- Number of turns: 100
- Effective coil area: 113.04 m²

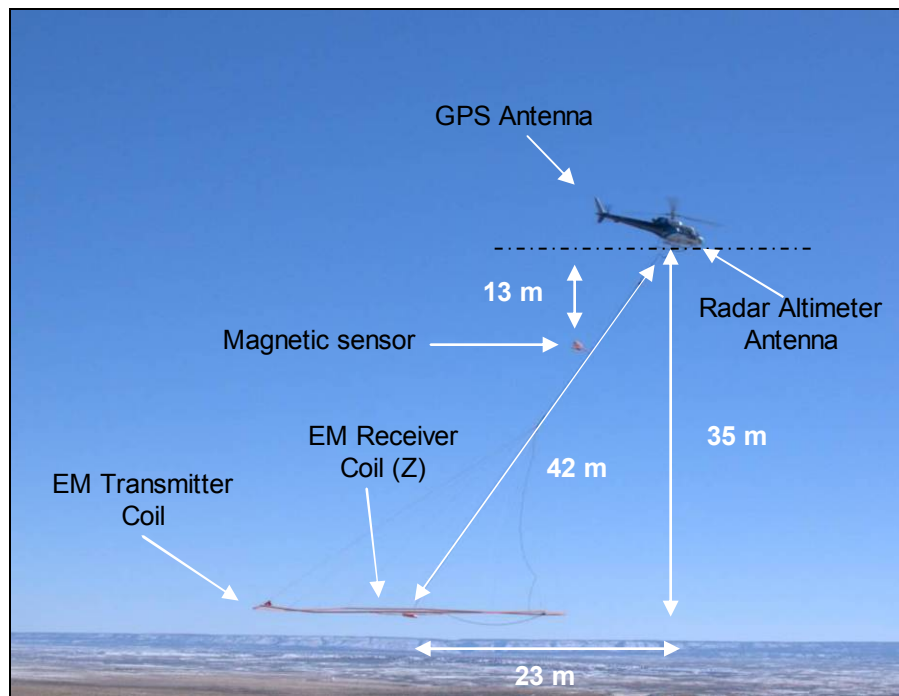


Figure 6: VTEM System Configuration.

2.4.3 Airborne magnetometer

The magnetic sensor utilized for the survey was Geometrics optically pumped caesium vapour magnetic field sensor mounted 13 metres below the helicopter, as shown in Figure 6. The sensitivity of the magnetic sensor is 0.02 nanoTesla (nT) at a sampling interval of 0.1 seconds.

2.4.4 Radar Altimeter

A Terra TRA 3000/TRI 40 radar altimeter was used to record terrain clearance. The antenna was mounted beneath the bubble of the helicopter cockpit (Figure 6).

2.4.5 GPS Navigation System

The navigation system used was a Geotech PC104 based navigation system utilizing a NovAtel's WAAS (Wide Area Augmentation System) enabled GPS receiver, Geotech navigate software, a full screen display with controls in front of the pilot to direct the flight and a NovAtel GPS antenna mounted on the helicopter tail (Figure 6). As many as 11 GPS and two WAAS satellites may be monitored at any one time. The positional accuracy or circular error probability (CEP) is 1.8 m, with WAAS active, it is 1.0 m. The co-ordinates of the block were set-up prior to the survey and the information was fed into the airborne navigation system.

2.4.6 Digital Acquisition System

A Geotech data acquisition system recorded the digital survey data on an internal compact flash card. Data is displayed on an LCD screen as traces to allow the operator to monitor the integrity of the system. The data type and sampling interval as provided in Table 4.

Table 4: Acquisition Sampling Rates

Data Type	Sampling
TDEM	0.1 sec
Magnetometer	0.1 sec
GPS Position	0.2 sec
Radar Altimeter	0.2 sec

2.5 Base Station

A combined magnetometer/GPS base station was utilized on this project. A Geometrics Cesium vapour magnetometer was used as a magnetic sensor with a sensitivity of 0.001 nT. The base station was recording the magnetic field together with the GPS time at 1 Hz on a base station computer.

The base station magnetometer sensor was installed ($61^{\circ} 48.6848'N$, $130^{\circ} 11.6767'W$); away from electric transmission lines and moving ferrous objects such as motor vehicles. The base station data were backed-up to the data processing computer at the end of each survey day.

3. PERSONNEL

The following Geotech Ltd. personnel were involved in the project.

Field:

Project Manager:	Darren Tuck (Office)
Data QC:	Neil Fiset (Office)
Crew chief:	Rick Gotuzzo
Operator:	Rick Gotuzzo

The survey pilot and the mechanical engineer were employed directly by the helicopter operator – Geotech Aviation.

Pilot:	Jocelyn Vallieres
--------	-------------------

Office:

Preliminary Data Processing:	Neil Fiset
Final Data Processing:	Marta Orta
Final Data QA/QC:	Geoffrey Plastow Alexander Prikhodko
Reporting/Mapping:	Wendy Acorn

Data acquisition phase was carried out under the supervision of Andrei Bagrianski, P. Geo, Chief Operations Officer. The processing and interpretation phase was under the supervision of Geoffrey Plastow, P. Geo, Data Processing Manager. The overall contract management and customer relations were by Mandy Long.

4. DATA PROCESSING AND PRESENTATION

Data compilation and processing were carried out by the application of Geosoft OASIS Montaj and programs proprietary to Geotech Ltd.

4.1 Flight Path

The flight path, recorded by the acquisition program as WGS 84 latitude/longitude, was converted into the NAD83 Datum, UTM Zone 9 North coordinate system in Oasis Montaj.

The flight path was drawn using linear interpolation between x, y positions from the navigation system. Positions are updated every second and expressed as UTM easting's (x) and UTM northing's (y).

4.2 Electromagnetic Data

A three stage digital filtering process was used to reject major spheric events and to reduce system noise. Local spheric activity can produce sharp, large amplitude events that cannot be removed by conventional filtering procedures. Smoothing or stacking will reduce their amplitude but leave a broader residual response that can be confused with geological phenomena. To avoid this possibility, a computer algorithm searches out and rejects the major spheric events.

The signal to noise ratio was further improved by the application of a low pass linear digital filter. This filter has zero phase shift which prevents any lag or peak displacement from occurring, and it suppresses only variations with a wavelength less than about 1 second or 15 metres. This filter is a symmetrical 1 sec linear filter.

The results are presented as stacked profiles of EM voltages for the time gates, in linear - logarithmic scale for the B-field Z component and dB/dt Z component responses. B-field Z component time channel recorded at 2.021 milliseconds for the Expo Block and 0.505 milliseconds for the Ellen Creek Block after the termination of the impulse is also presented as a color image. Calculated Time Constant (TAU) with Calculated Vertical Derivative contours is presented in Appendix C and E. Tau was calculated for B-Field and dB/dt. Resistivity Depth Image (RDI) is also presented in Appendix F and G.

VTEM receiver coil orientation Z-axis coil is oriented parallel to the transmitter coil axis and is horizontal to the ground. Generalized modeling results of VTEM data, are shown in Appendix D.

Z component data produce double peak type anomalies for "thin" subvertical targets and single peak for "thick" targets.

The limits and change-over of "thin-thick" depends on dimensions of a TEM system the system's height and depth of a target. For example see Appendix D, Fig.D-16.

4.3 Magnetic Data

The processing of the magnetic data involved the correction for diurnal variations by using the digitally recorded ground base station magnetic values. The base station magnetometer data was edited and merged into the Geosoft GDB database on a daily basis. The aeromagnetic data was corrected for diurnal variations by subtracting the observed magnetic base station deviations.

Tie line levelling was carried out by adjusting intersection points along traverse lines. A micro-levelling procedure was applied to remove persistent low-amplitude components of flight-line noise remaining in the data.

The corrected magnetic data was interpolated between survey lines using a random point gridding method to yield x-y grid values for a standard grid cell size of 25 metres at the mapping scale. The Minimum Curvature algorithm was used to interpolate values onto a rectangular regular spaced grid.

5. DELIVERABLES

5.1 Survey Report

The survey report describes the data acquisition, processing, and final presentation of the survey results. The survey report is provided in two paper copies and digitally in PDF format.

5.2 Maps

Final maps were produced at scale of 1:10,000 for best representation of the survey size and line spacing. The coordinate/projection system used was NAD83 Datum, UTM Zone 9 North. All maps show the flight path trace and topographic data; latitude and longitude are also noted on maps.

The preliminary and final results of the survey are presented as EM profiles, a late-time gate gridded EM channel, and a colour magnetic TMI contour map.

- Maps at 1:10,000 in Geosoft MAP format, as follows:
 - GL140269_10K_dBdt_bb: dB/dt profiles Z Component, Time Gates 0.220 – 7.036 ms in linear – logarithmic scale.
 - GL140269_10K_Bfield_bb: B-field profiles Z Component, Time Gates 0.220 – 7.036 ms in linear – logarithmic scale.
 - GL140269_10K_BFz36_bb: B-Field late time Z Component Channel 36, Time Gate 2.021 ms colour image.
 - GL140269_10K_BFz26_bb: B-Field late time Z Component Channel 26, Time Gate 0.505 ms colour image.
 - GL140269_10K_TMI_bb: Total Magnetic Intensity (TMI) colour image and contours.
 - GL140269_10K_TauSF_bb: dB/dt Calculated Time Constant (TAU) with Calculated Vertical Derivative contours.

Where bb represents the block name ie GL140269_10k_TMI_Expo

Maps are also presented in PDF format.

- 1:50,000 topographic vectors were taken from the NRCAN Geogratis database at: <http://geogratis.gc.ca/geogratis/en/index.html>.
- A Google Earth file *GL140269_Yukon.kml* showing the flight path of the survey area is included. Free versions of Google Earth software from: <http://earth.google.com/download-earth.html>

5.3 Digital Data

- Two copies of the data and maps on DVD were prepared to accompany the report. Each DVD contains a digital file of the line data in GDB Geosoft Montaj format as well as the maps in Geosoft Montaj Map and PDF format.
- DVD structure.

Data contains databases, grids and maps, as described below.

Report contains a copy of the report and appendices in PDF format.

Databases in Geosoft GDB format, containing the channels listed in Table 5.

Table 5: Geosoft GDB Data Format

Channel name	Units	Description
X:	metres	UTM Easting NAD83 Zone 9 North
Y:	metres	UTM Northing NAD83 Zone 9 North
Longitude:	Decimal Degrees	WGS 84 Longitude data
Latitude:	Decimal Degrees	WGS 84 Latitude data
Z:	metres	GPS antenna elevation (above Geoid)
Zb:	metres	Transmitter-receiver loop elevation (above Geoid)
Radar:	metres	helicopter terrain clearance from radar altimeter
Radarb:	metres	Calculated EM bird terrain clearance from radar altimeter
DEM:	metres	Digital Elevation Model
Gtime:	Seconds of the day	GPS time
Mag1:	nT	Raw Total Magnetic field data
Basemag:	nT	Magnetic diurnal variation data
Mag2:	nT	Diurnal corrected Total Magnetic field data
Mag3:	nT	Levelled Total Magnetic field data
CVG	nT/m	Calculated Magnetic Vertical Gradient
SFz[14]:	$\text{pV}/(\text{A} \cdot \text{m}^4)$	Z dB/dt 0.096 millisecond time channel
SFz[15]:	$\text{pV}/(\text{A} \cdot \text{m}^4)$	Z dB/dt 0.110 millisecond time channel
SFz[16]:	$\text{pV}/(\text{A} \cdot \text{m}^4)$	Z dB/dt 0.126 millisecond time channel
SFz[17]:	$\text{pV}/(\text{A} \cdot \text{m}^4)$	Z dB/dt 0.145 millisecond time channel
SFz[18]:	$\text{pV}/(\text{A} \cdot \text{m}^4)$	Z dB/dt 0.167 millisecond time channel
SFz[19]:	$\text{pV}/(\text{A} \cdot \text{m}^4)$	Z dB/dt 0.192 millisecond time channel
SFz[20]:	$\text{pV}/(\text{A} \cdot \text{m}^4)$	Z dB/dt 0.220 millisecond time channel
SFz[21]:	$\text{pV}/(\text{A} \cdot \text{m}^4)$	Z dB/dt 0.253 millisecond time channel
SFz[22]:	$\text{pV}/(\text{A} \cdot \text{m}^4)$	Z dB/dt 0.290 millisecond time channel
SFz[23]:	$\text{pV}/(\text{A} \cdot \text{m}^4)$	Z dB/dt 0.333 millisecond time channel
SFz[24]:	$\text{pV}/(\text{A} \cdot \text{m}^4)$	Z dB/dt 0.383 millisecond time channel
SFz[25]:	$\text{pV}/(\text{A} \cdot \text{m}^4)$	Z dB/dt 0.440 millisecond time channel
SFz[26]:	$\text{pV}/(\text{A} \cdot \text{m}^4)$	Z dB/dt 0.505 millisecond time channel
SFz[27]:	$\text{pV}/(\text{A} \cdot \text{m}^4)$	Z dB/dt 0.580 millisecond time channel
SFz[28]:	$\text{pV}/(\text{A} \cdot \text{m}^4)$	Z dB/dt 0.667 millisecond time channel
SFz[29]:	$\text{pV}/(\text{A} \cdot \text{m}^4)$	Z dB/dt 0.766 millisecond time channel
SFz[30]:	$\text{pV}/(\text{A} \cdot \text{m}^4)$	Z dB/dt 0.880 millisecond time channel
SFz[31]:	$\text{pV}/(\text{A} \cdot \text{m}^4)$	Z dB/dt 1.010 millisecond time channel
SFz[32]:	$\text{pV}/(\text{A} \cdot \text{m}^4)$	Z dB/dt 1.161 millisecond time channel
SFz[33]:	$\text{pV}/(\text{A} \cdot \text{m}^4)$	Z dB/dt 1.333 millisecond time channel

Channel name	Units	Description
SFz[34]:	$\mu\text{V}/(\text{A}\cdot\text{m}^4)$	Z dB/dt 1.531 millisecond time channel
SFz[35]:	$\mu\text{V}/(\text{A}\cdot\text{m}^4)$	Z dB/dt 1.760 millisecond time channel
SFz[36]:	$\mu\text{V}/(\text{A}\cdot\text{m}^4)$	Z dB/dt 2.021 millisecond time channel
SFz[37]:	$\mu\text{V}/(\text{A}\cdot\text{m}^4)$	Z dB/dt 2.323 millisecond time channel
SFz[38]:	$\mu\text{V}/(\text{A}\cdot\text{m}^4)$	Z dB/dt 2.667 millisecond time channel
SFz[39]:	$\mu\text{V}/(\text{A}\cdot\text{m}^4)$	Z dB/dt 3.063 millisecond time channel
SFz[40]:	$\mu\text{V}/(\text{A}\cdot\text{m}^4)$	Z dB/dt 3.521 millisecond time channel
SFz[41]:	$\mu\text{V}/(\text{A}\cdot\text{m}^4)$	Z dB/dt 4.042 millisecond time channel
SFz[42]:	$\mu\text{V}/(\text{A}\cdot\text{m}^4)$	Z dB/dt 4.641 millisecond time channel
SFz[43]:	$\mu\text{V}/(\text{A}\cdot\text{m}^4)$	Z dB/dt 5.333 millisecond time channel
SFz[44]:	$\mu\text{V}/(\text{A}\cdot\text{m}^4)$	Z dB/dt 6.125 millisecond time channel
SFz[45]:	$\mu\text{V}/(\text{A}\cdot\text{m}^4)$	Z dB/dt 7.036 millisecond time channel
SFz[46]:	$\mu\text{V}/(\text{A}\cdot\text{m}^4)$	Z dB/dt 8.083 millisecond time channel
SFz[47]:	$\mu\text{V}/(\text{A}\cdot\text{m}^4)$	Z dB/dt 9.286 millisecond time channel
SFz[48]:	$\mu\text{V}/(\text{A}\cdot\text{m}^4)$	Z dB/dt 10.667 millisecond time channel
BFz	$(\mu\text{V}\cdot\text{ms})/(\text{A}\cdot\text{m}^4)$	Z B-Field data for time channels 14 to 48
PLM:		60 Hz power line monitor
TauSF	milliseconds	Time Constant (Tau) calculated from dB/dt data
Nchan_SF		Last channel where the Tau algorithm stops calculation, dB/dt data
TauBF	milliseconds	Time Constant (Tau) calculated from B-Field data
Nchan_BF		Last channel where the Tau algorithm stops calculation, B-Field data

Electromagnetic B-field and dB/dt Z component data is found in array channel format between indexes 14 – 48

- Database of the Resistivity Depth Images in Geosoft GDB format, containing the following channels:

Table 6: Geosoft Resistivity Depth Image GDB Data Format

Channel name	Units	Description
Xg:	metres	UTM Easting NAD83 Zone 9 North
Yg:	metres	UTM Northing NAD83 Zone 9 North
Dist:	meters	Distance from the beginning of the line
Depth:	meters	array channel, depth from the surface
Z:	meters	array channel, depth from sea level
AppRes:	Ohm-m	array channel, Apparent Resistivity
TR:	meters	EM system height from sea level
Topo:	meters	digital elevation model
Radarb:	metres	Calculated EM bird terrain clearance from radar altimeter
SF:	$\mu\text{V}/(\text{A}\cdot\text{m}^4)$	array channel, dB/dT
Mag:	nT	Total Magnetic field data
CVG:	nT/m	CVG data
DOI:	metres	Depth of Investigation: a measure of VTEM depth effectiveness

- Database of the VTEM Waveform “GL140269_waveform_final.gdb” in Geosoft GDB format, contains the channels described in Table 7

Table 7: Geosoft database for the VTEM waveform

Channel name	Description
Time:	Sampling rate interval, 5.2083 microseconds
Tx Current:	Output current of the transmitter (amps)
Rx Voltage:	Output voltage of the receiver coil (volts)

- Grids in Geosoft GRD and GeoTIFF format, as follows:

BFz26: B-Field Z Component Channel 26 (Time Gate 0.505 ms)
 BFz36: B-Field Z Component Channel 36 (Time Gate 2.021 ms)
 CVG: Calculated Vertical Derivative of TMI (CVG)
 DEM: Digital Elevation Model
 Mag3: Total Magnetic Intensity (TMI)
 PLM: Power line Monitor
 SFz15: dB/dt Z Component Channel 15 (Time Gate 0.110 ms)
 SFz30: dB/dt Z Component Channel 30 (Time Gate 0.880 ms)
 SFz40: dB/dt Z Component Channel 40 (Time Gate 3.521 ms)
 TauSF: dB/dt Calculated Time Constant (TAU)
 TauBF: B-Field Calculated Time Constant (TAU)

A Geosoft .GRD file has a .GI metadata file associated with it, containing grid projection information. A grid cell size of 25 metres was used.

6. CONCLUSIONS AND RECOMMENDATIONS

A helicopter-borne versatile time domain electromagnetic (VTEM) geophysical survey has been completed over the Expo and Ellen Creek Blocks near Finlayson Lake, Yukon.

The total area coverage is 53 km². Total survey line coverage is 579 line kilometres. The principal sensors included a Time Domain EM system and a magnetometer. Results have been presented as stacked profiles, and contour color images at a scale of 1:10,000. A formal Interpretation has not been included or requested.

Based on the geophysical results obtained, a number of TEM anomalies are identified in the blocks. These conductive targets are highlighted in the Tau decay parameter image with calculated vertical magnetic gradient (CVG) contours, presented in Figures 7 below. Resistivity-depth images (RDI) are selected for discussion, and are also highlighted in figure below.

Expo block

The strongest conductive response is observed toward the middle-south part of the block (Tau calculated from dBz/dt data is up to 2.3 ms).

A conductor is observed between lines L1320 to L1360 and tie-line T2060 (anomaly A in figure below). This conductor is located in the east border of a high topography. Apparent resistivity is < 23 ohm-m according to RDI results of L1320. Minimal association to magnetic anomalies is observed at this location (436,591m easting).

A conductive zone is observed in the south-west part of the block trending NE-SW exhibiting a double-peak anomaly between lines L1390 to L1480 (anomaly B1). This conductive zone widens and become more complex as it extends to the south up to line L1680 (anomaly B2) changing its trend to NW-SE. Apparent resistivity is < 10 ohm-m according to RDI results on L1540. This conductive zone of complex geometry is also seen in tie-lines T2000 and T2010.

Conductors C and D are observed in the centre-south part of the block between lines L1460 to L1570 and tie-lines T2050 (D) and T2060 (C). According to RDI of L1480, apparent resistivity is < 9 ohm-m where conductor C exhibits a single-peak anomaly (436,550m easting). At this location conductor C exhibits values of Tau up to 1.7 ms.

Conductor D is located in a zone with minimal association to magnetic anomalies, and appears to be induced by very-low conductive targets (Tau < 0.85 ms).

A conductive zone trending NE-SW is observed toward the south-east part of the block (anomaly E). A double-peak anomaly between lines L1570 to L1680 indicates that a sub-vertical conductor dipping to the west is associated to magnetic anomalies. On line L1640, the top of this conductor is located in 438,254m easting. Apparent resistivity is < 14 ohm-m according to RDI results of L1640.

Conductive trends in the north part of the Expo block appear to be induced by very-low conductive targets (Tau calculated from dBz/dt data is < 1 ms) that are attributed to lithology.

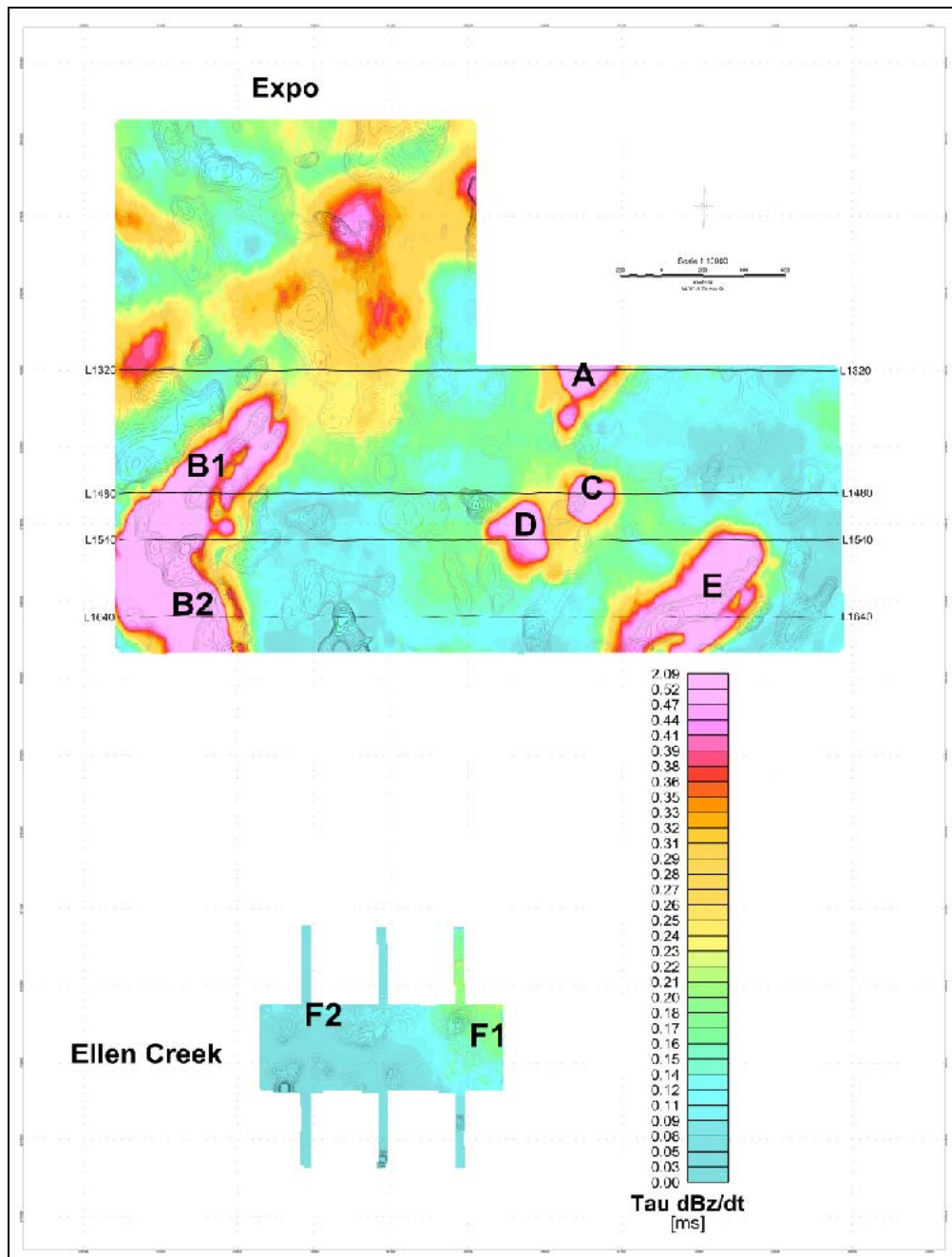


Figure 7: Image of time-constant (Tau calculated from dBz/dt data) with contours of the calculated vertical magnetic gradient (CVG of TMI).

Ellen Creek block

A conductive zone is observed in the east part of the block (anomaly F1 in figure above) induced by very-low conductive targets (Tau calculated from dBz/dt data is up to 0.48 ms). This conductive zone diminishes as it extends to the north-west part (F2). Apparent resistivity is about 171 ohm-m, according to RDI results.

As the conductors correspond to the exploration model of interest, it is recommended additional interpretation to be performed prior to ground follow up and drill testing, consisting of:

- 1) EM anomaly picking with target centre localization, conductance grading and depth estimation;
- 2) Resistivity depth slices at several level of depth;
- 3) Maxwell plate modelling of selected targets.

If magnetic anomalies are of interest, 3D inversion and/or modeling of the magnetic field are recommended as well.

Respectfully submitted²,



Neil Fiset
Geotech Ltd.



Marta Orta
Geotech Ltd.



Geoffrey Plastow, P. Geo
Data Processing Manager
Geotech Ltd.

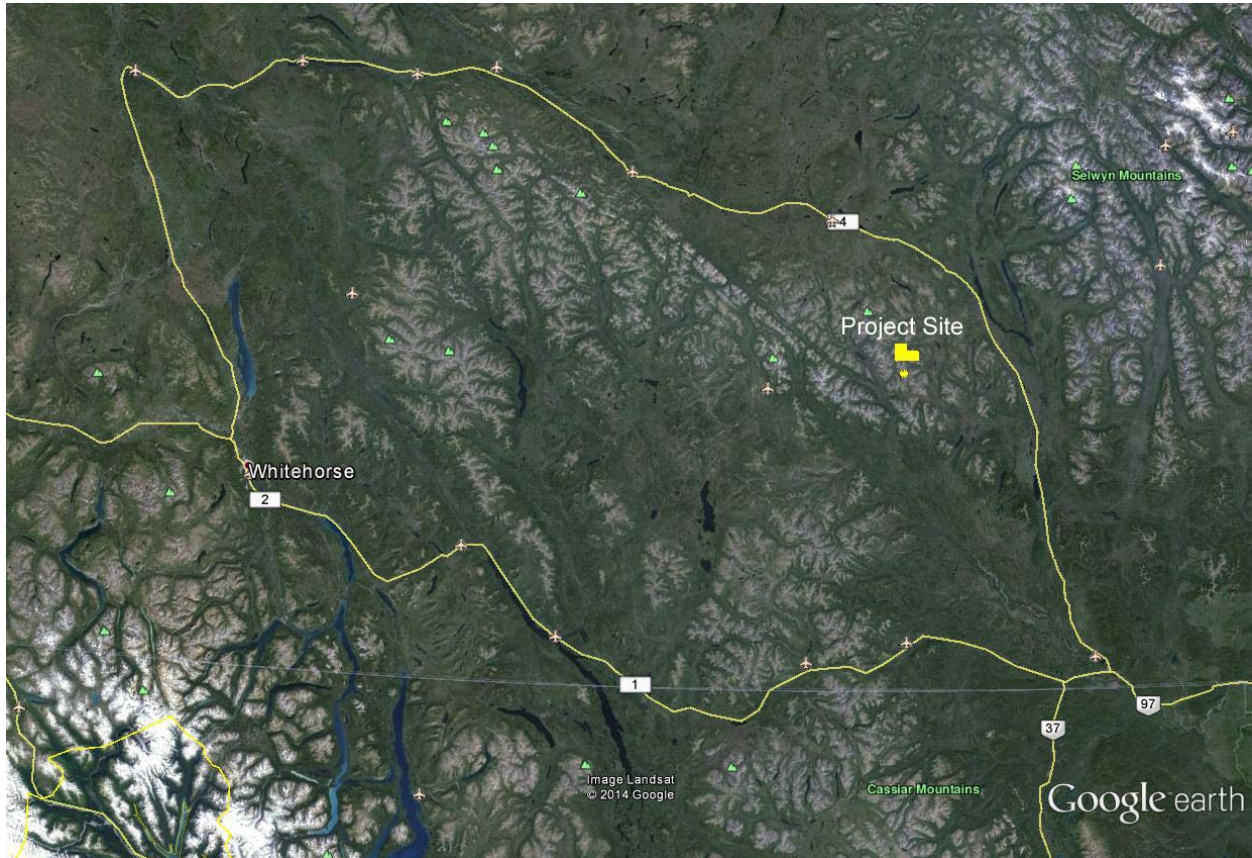


October 2014

² Final data processing of the EM and magnetic data were carried out by Marta Orta, from the office of Geotech Ltd. in Aurora, Ontario, under the supervision of Geoffrey Plastow, P. Geo., Data Processing Manager.

APPENDIX A

SURVEY AREA LOCATION MAP



Survey Overview

APPENDIX B

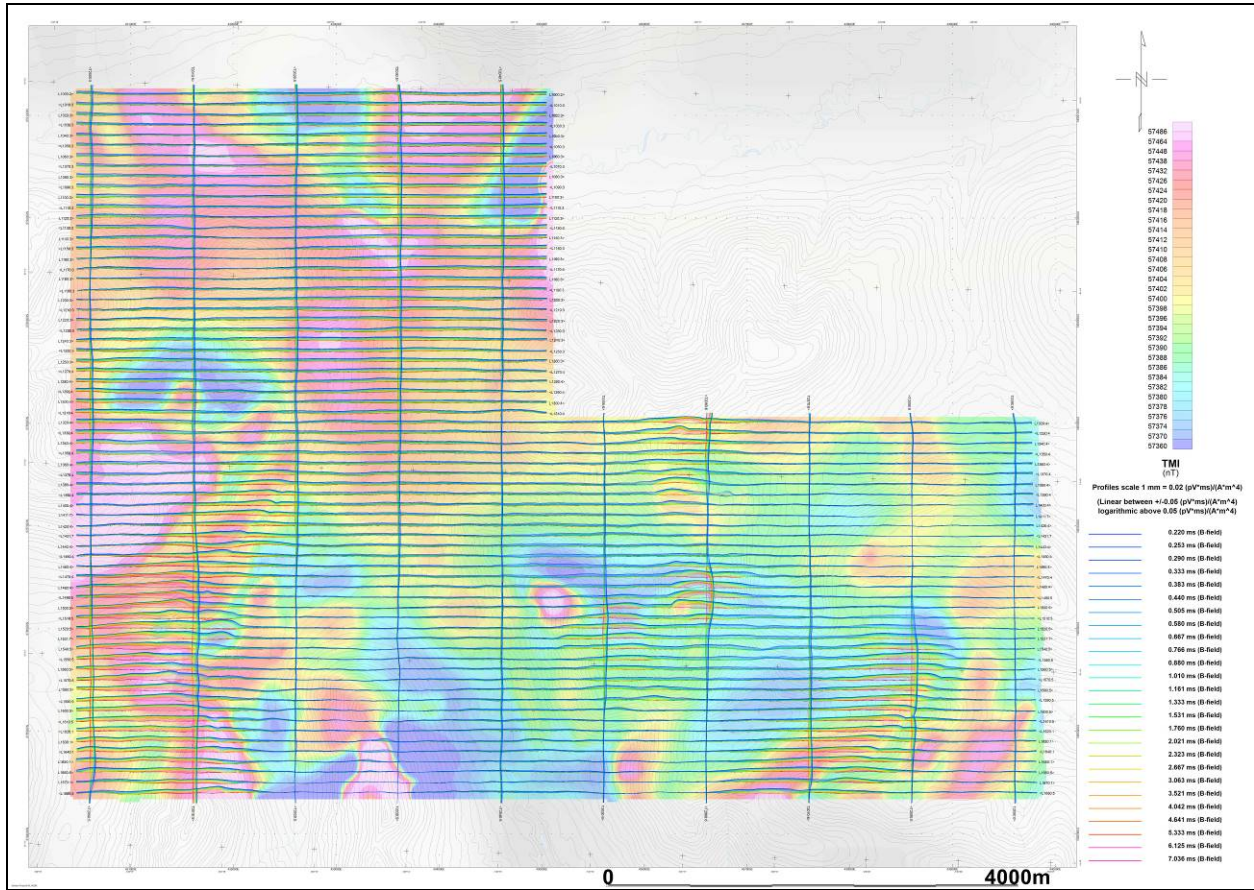
SURVEY BLOCK COORDINATES (WGS 84, UTM Zone 9 North)

Expo	
X	Y
430519	6784375
430519	6791211
435000	6791211
435000	6788000
439725	6788000
439774	6784375

Ellen Creek	
X	Y
432393	6778695
435393	6778695
435393	6779695
432393	6779695

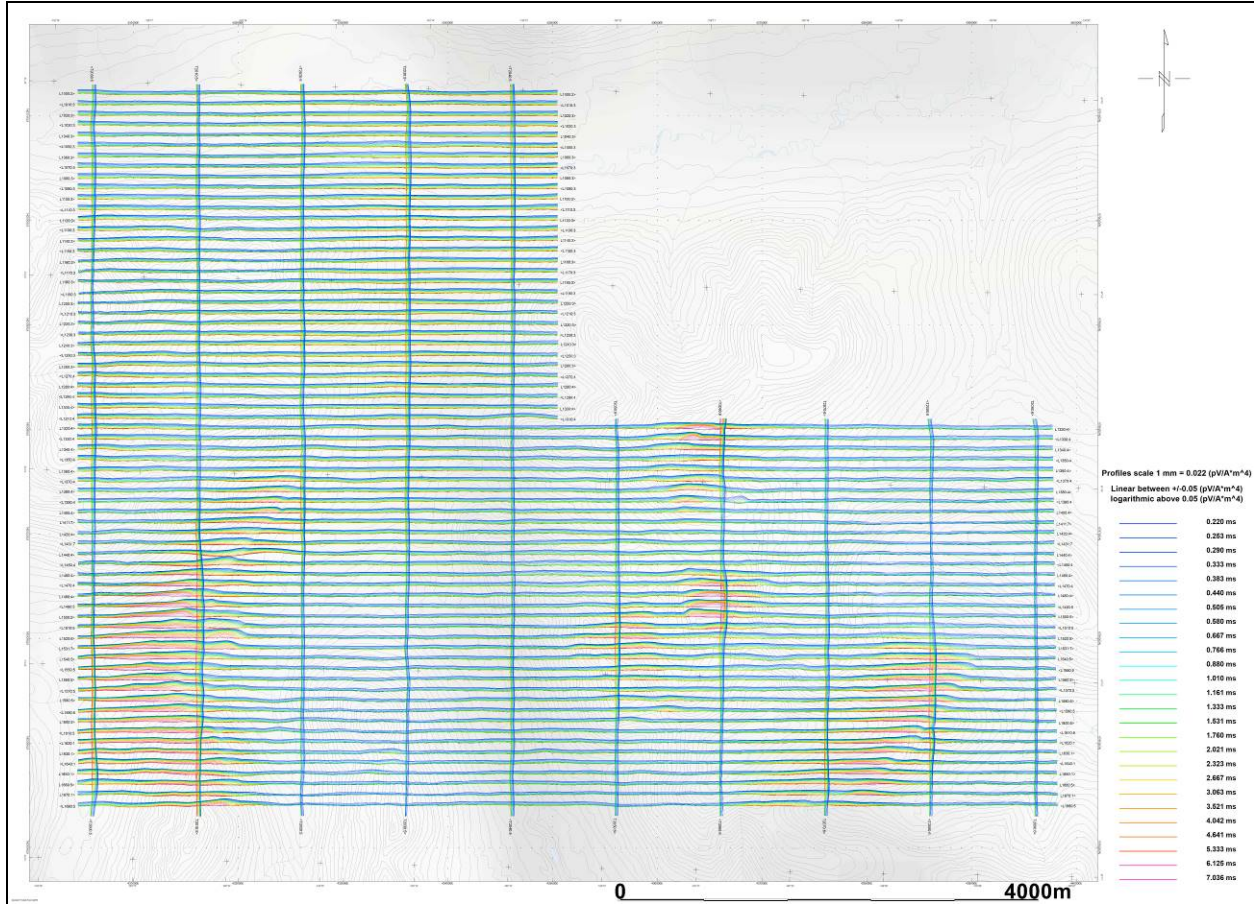
APPENDIX C

GEOPHYSICAL MAPS¹

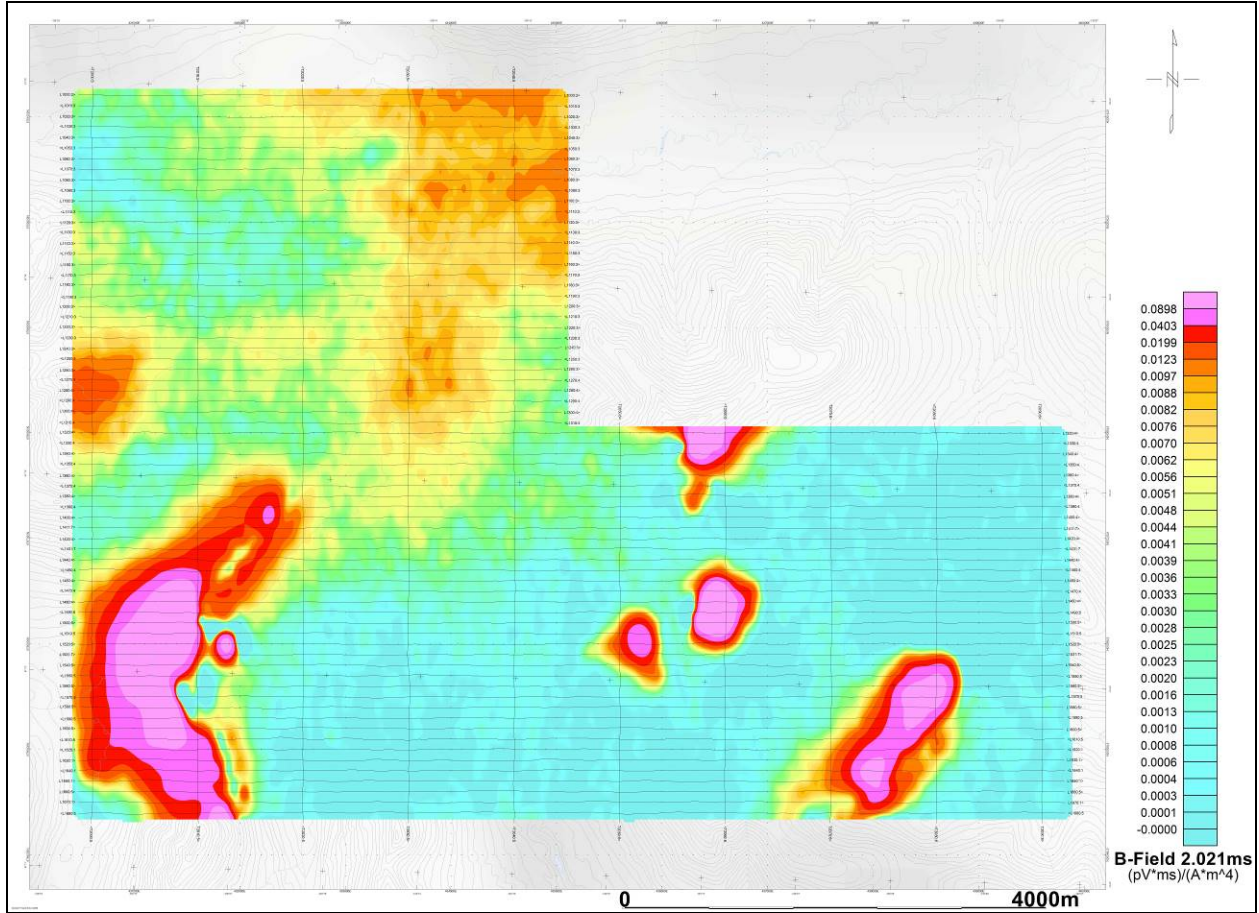


VTEM B-Field Z Component Profiles, Time Gates 0.220 to 7.036 ms – Expo Block

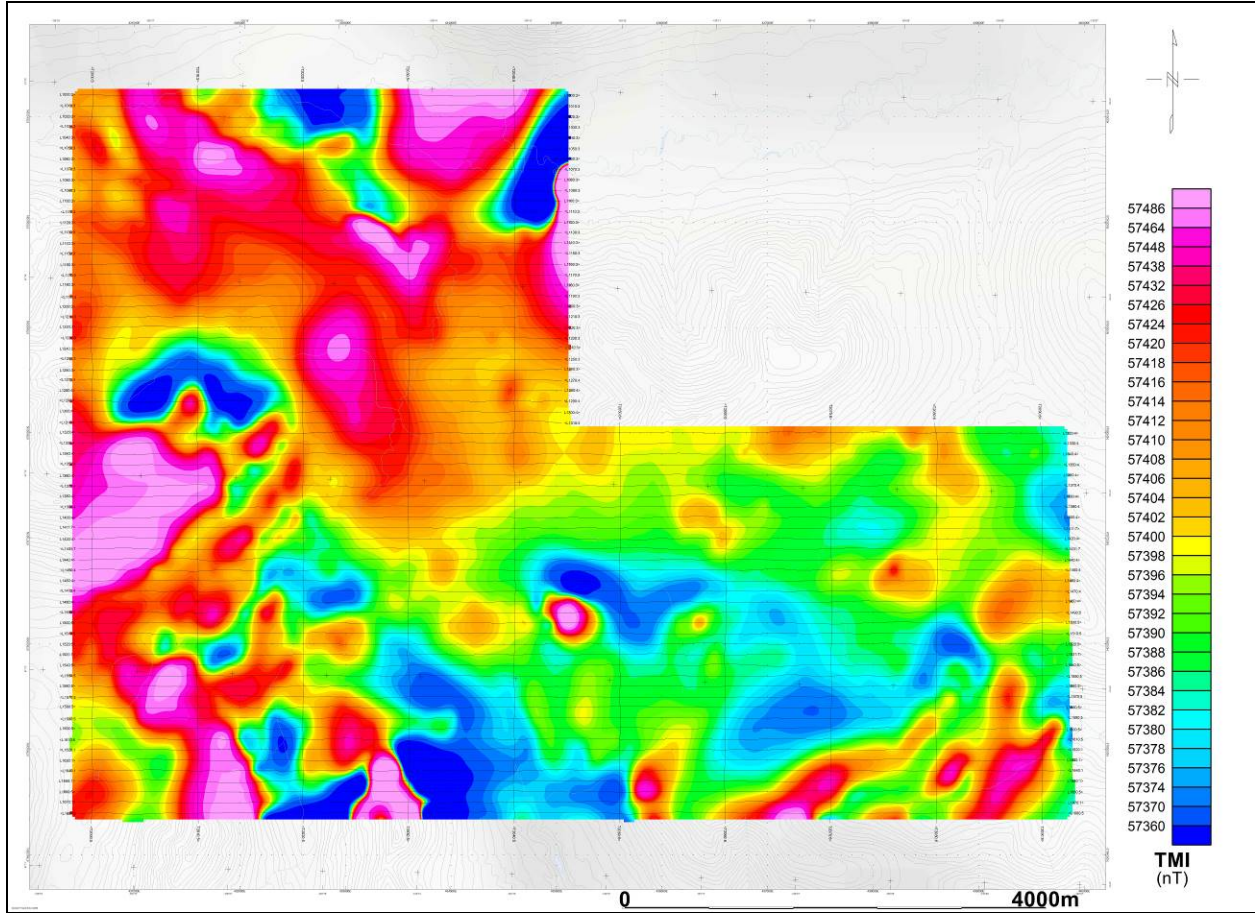
¹ Full size geophysical maps are also available in PDF format on the final DVD



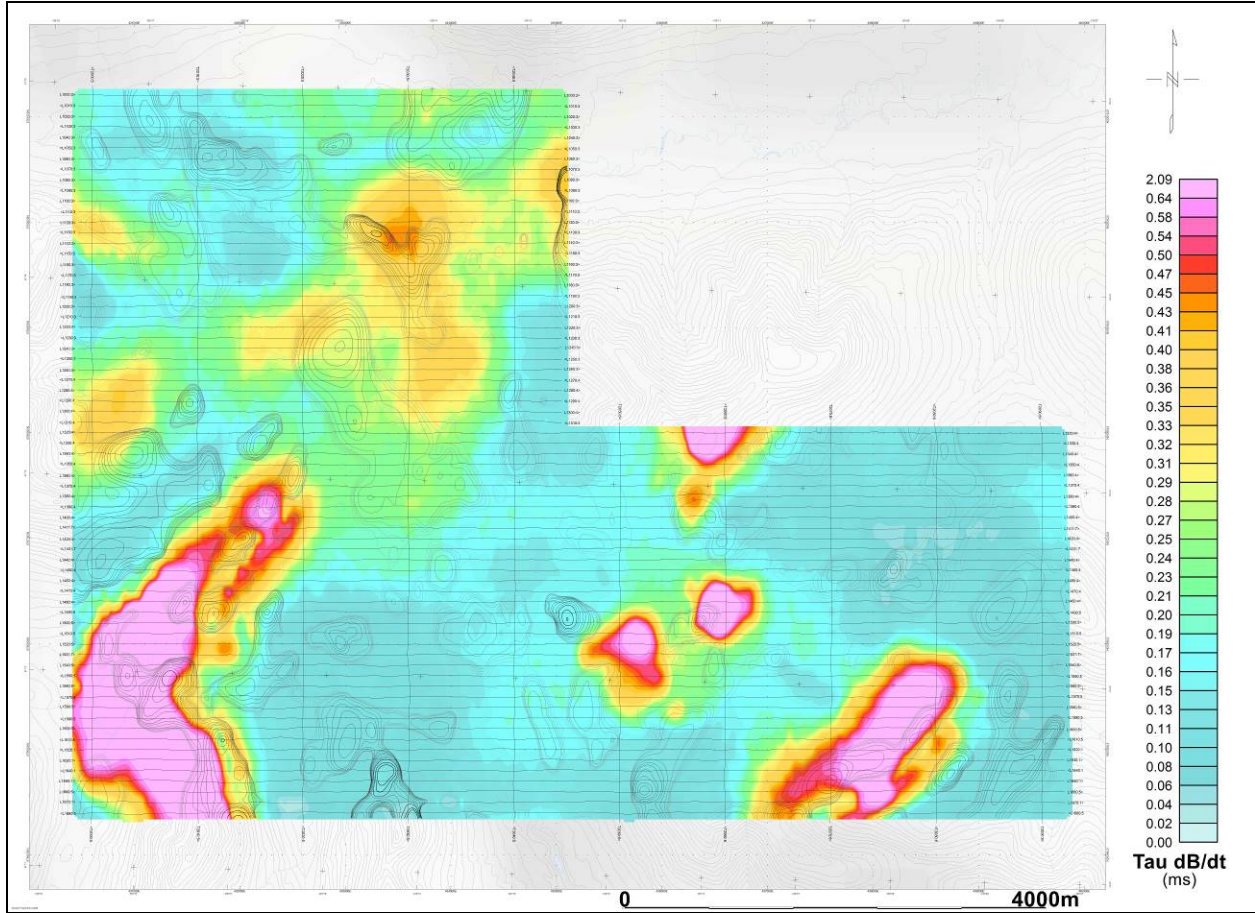
VTEM dB/dt Z Component Profiles, Time Gates 0.220 to 7.036 ms – Expo Block



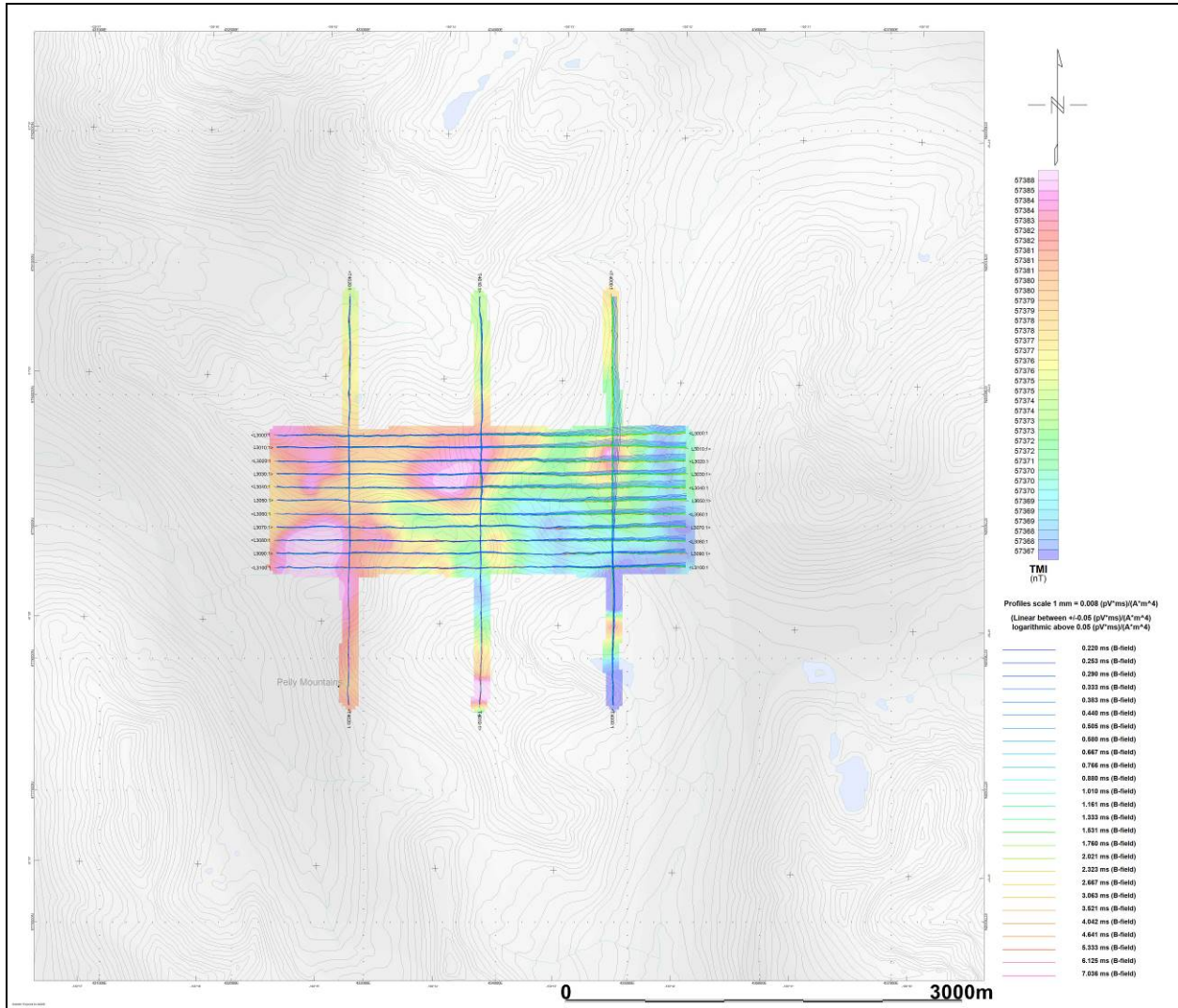
VTEM B-Field Channel 36, Time Gate 2.021 ms – Expo Block



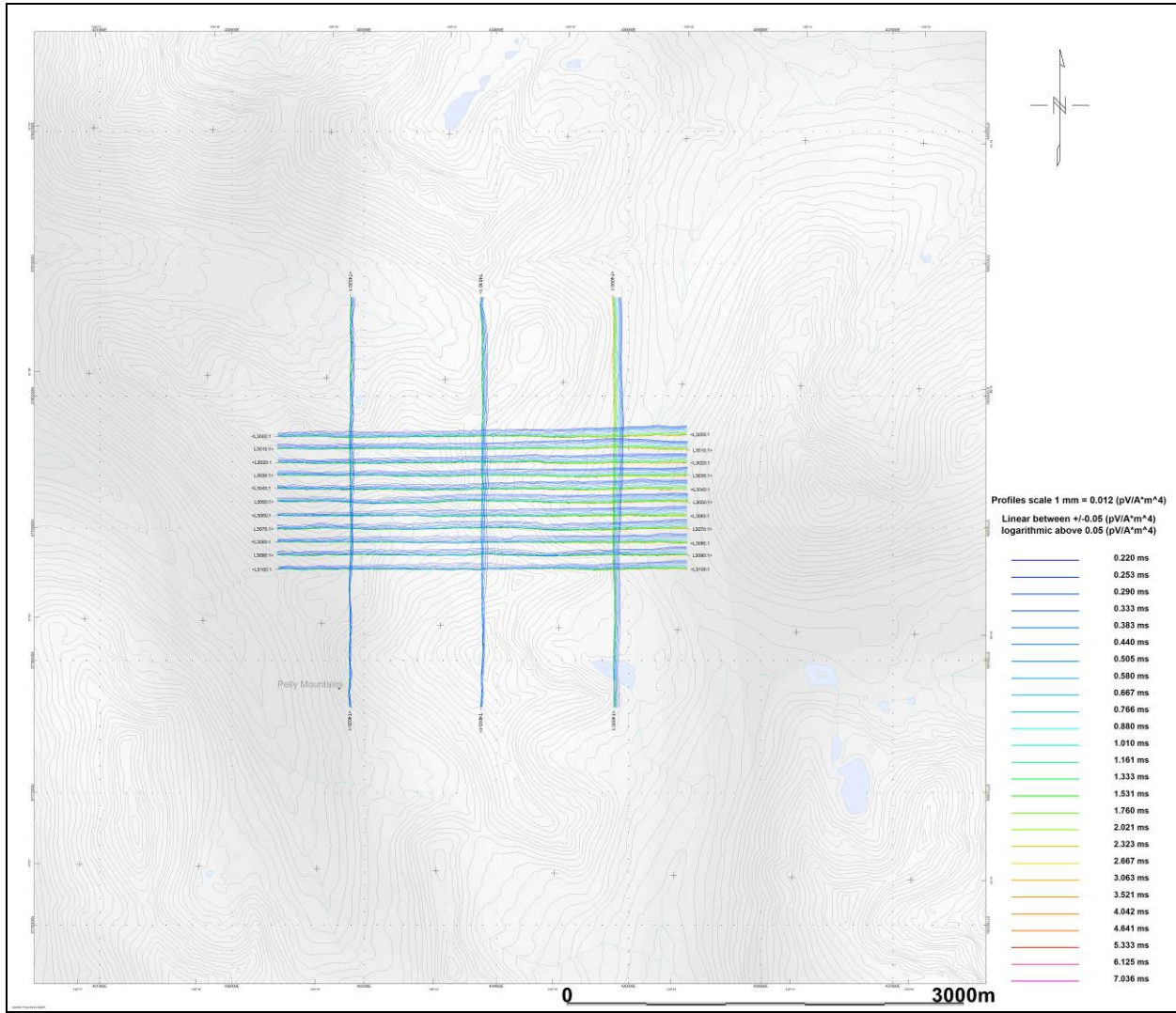
Total Magnetic Intensity – Expo Block



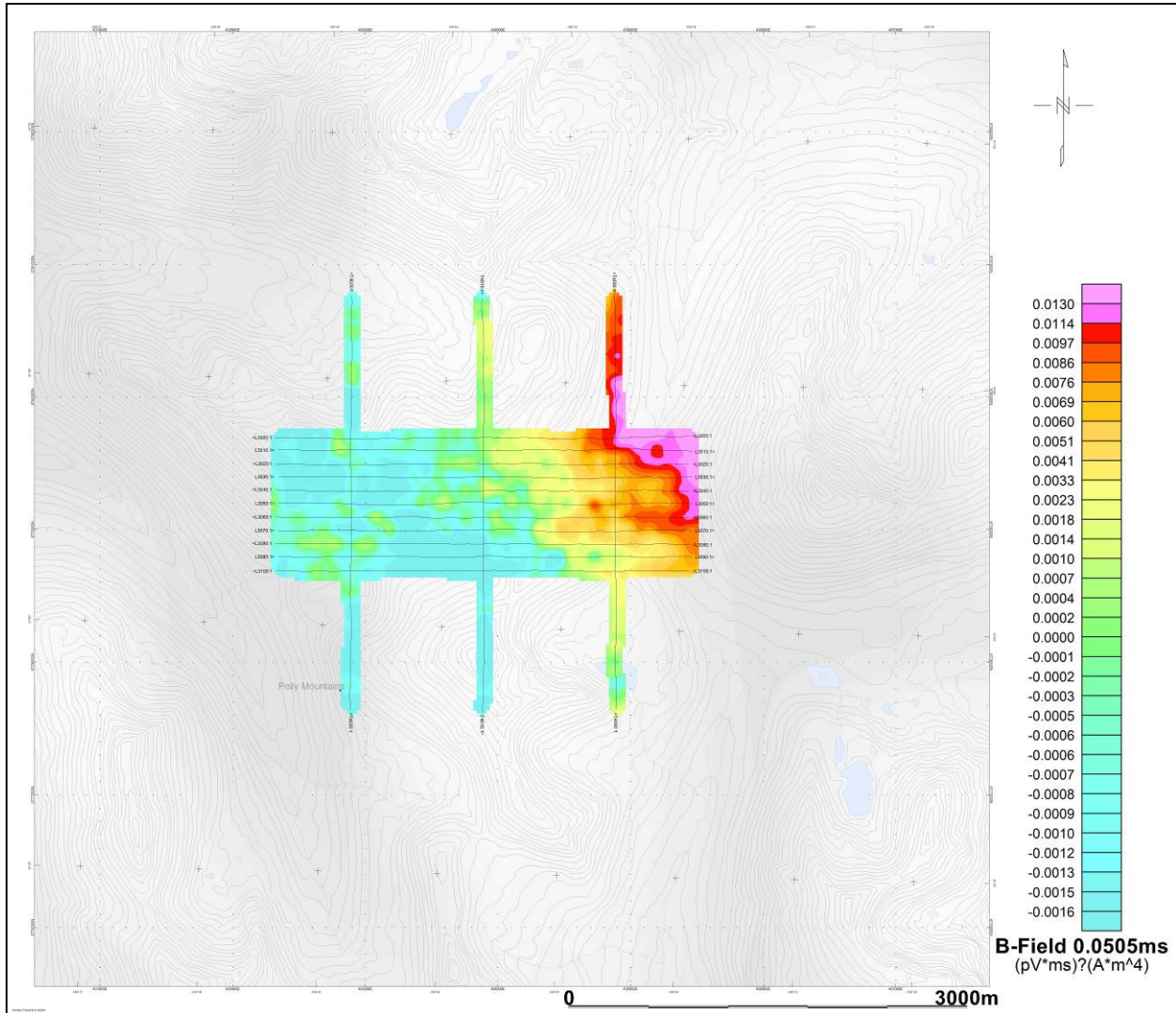
VTEM dB/dt Calculated Time Constant (TAU) with Calculated Vertical Derivative contours – Expo Block



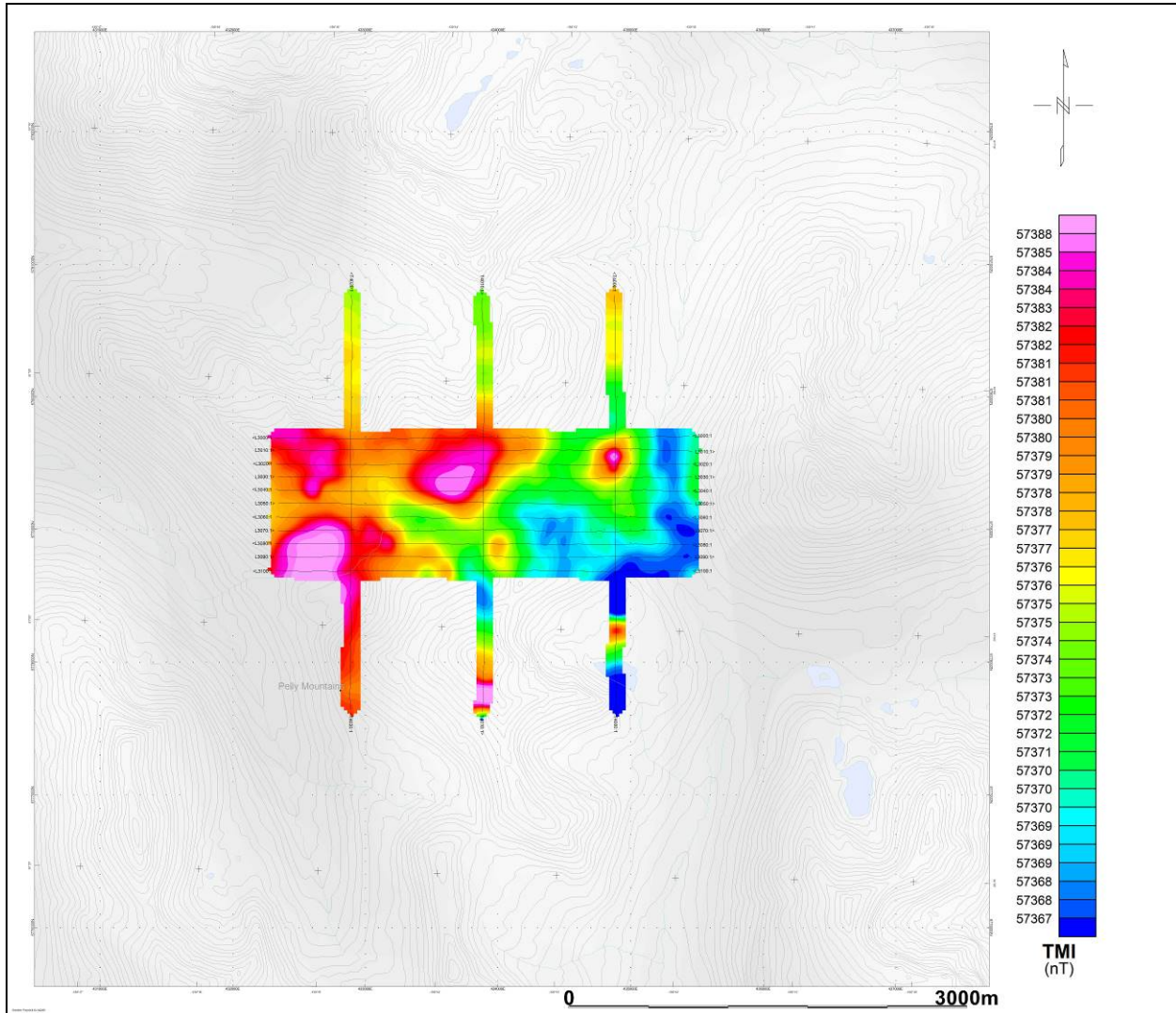
VTEM B-Field Z Component Profiles, Time Gates 0.220 to 7.036 ms – Ellen Creek Block



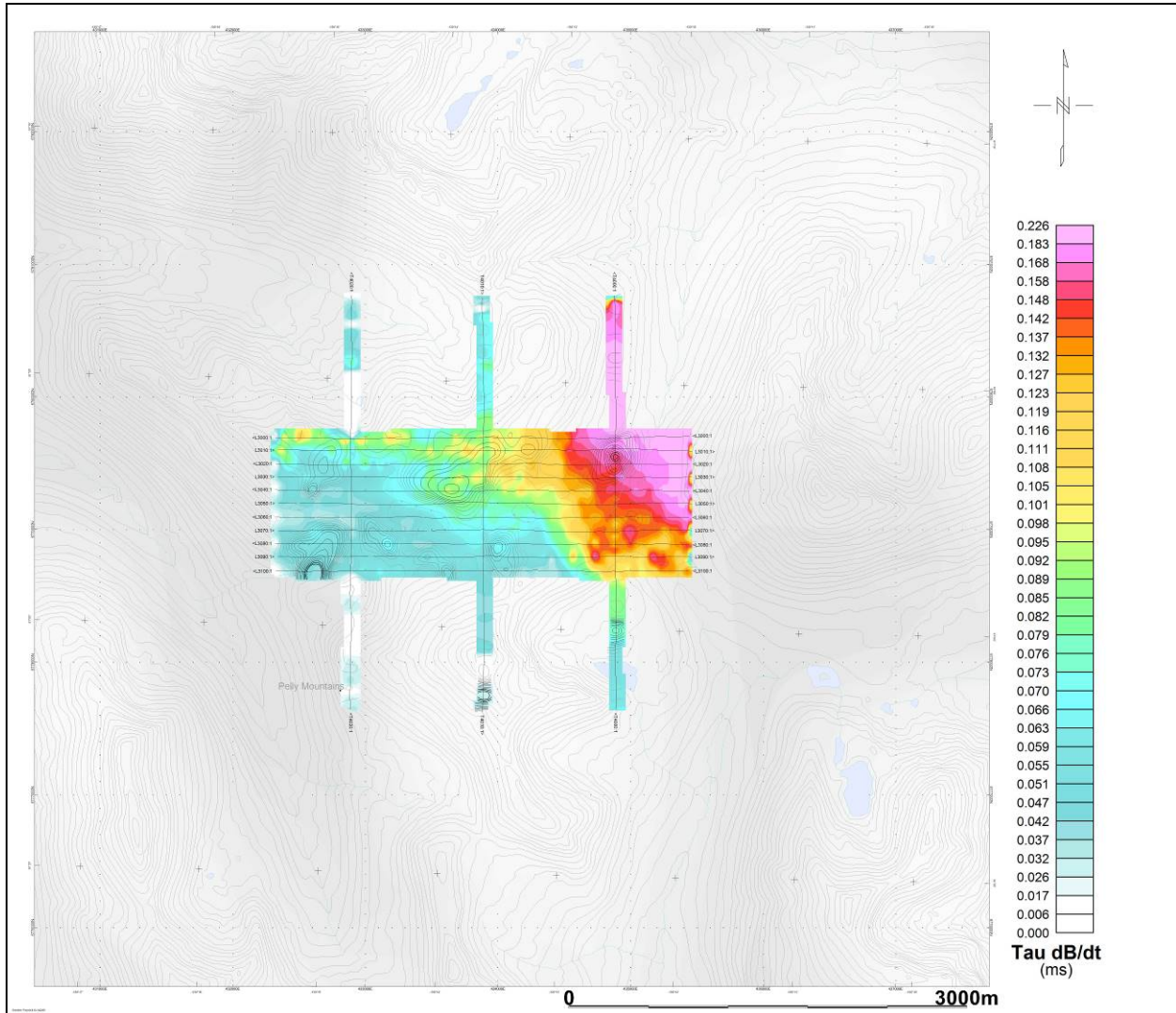
VTEM dB/dt Z Component Profiles, Time Gates 0.220 to 7.036 ms – Ellen Creek Block



VTEM B-Field Channel 26, Time Gate 0.505 ms – Ellen Creek Block



Total Magnetic Intensity – Ellen Creek Block

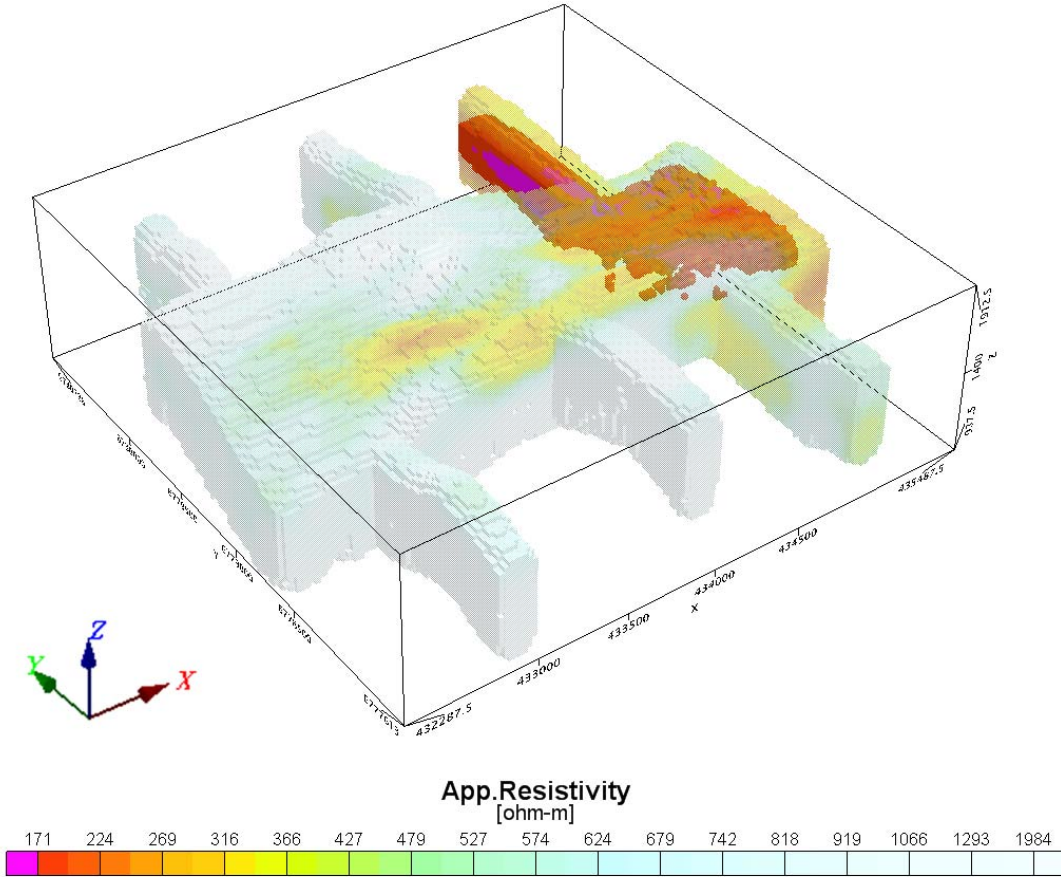


VTEM dB/dt Calculated Time Constant (TAU) with Calculated Vertical Derivative contours – Ellen Creek Block

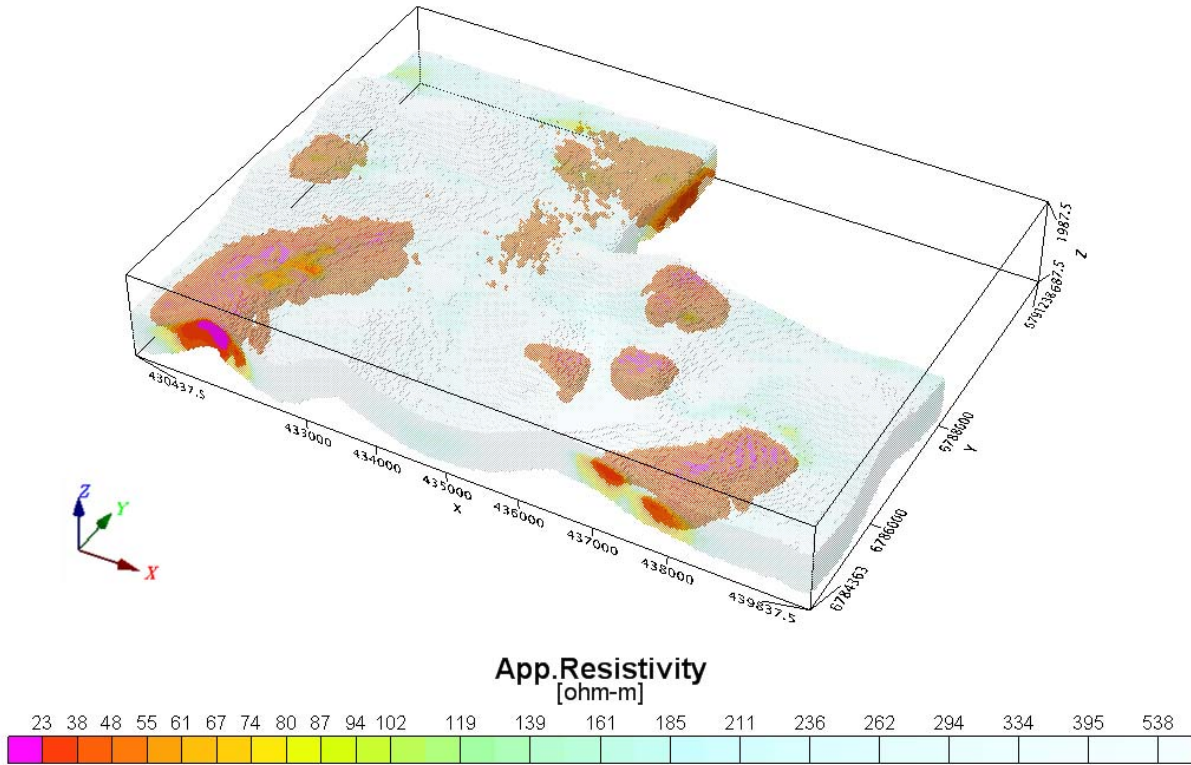
RESISTIVITY DEPTH IMAGE (RDI) MAPS

3D Resistivity Depth Image (RDI)

Apparent Resistivity Ellen Creek block



Apparent Resistivity Expo block



APPENDIX D

GENERALIZED MODELING RESULTS OF THE VTEM SYSTEM

Introduction

The VTEM system is based on a concentric or central loop design, whereby, the receiver is positioned at the centre of a transmitter loop that produces a primary field. The wave form is a bi-polar, modified square wave with a turn-on and turn-off at each end.

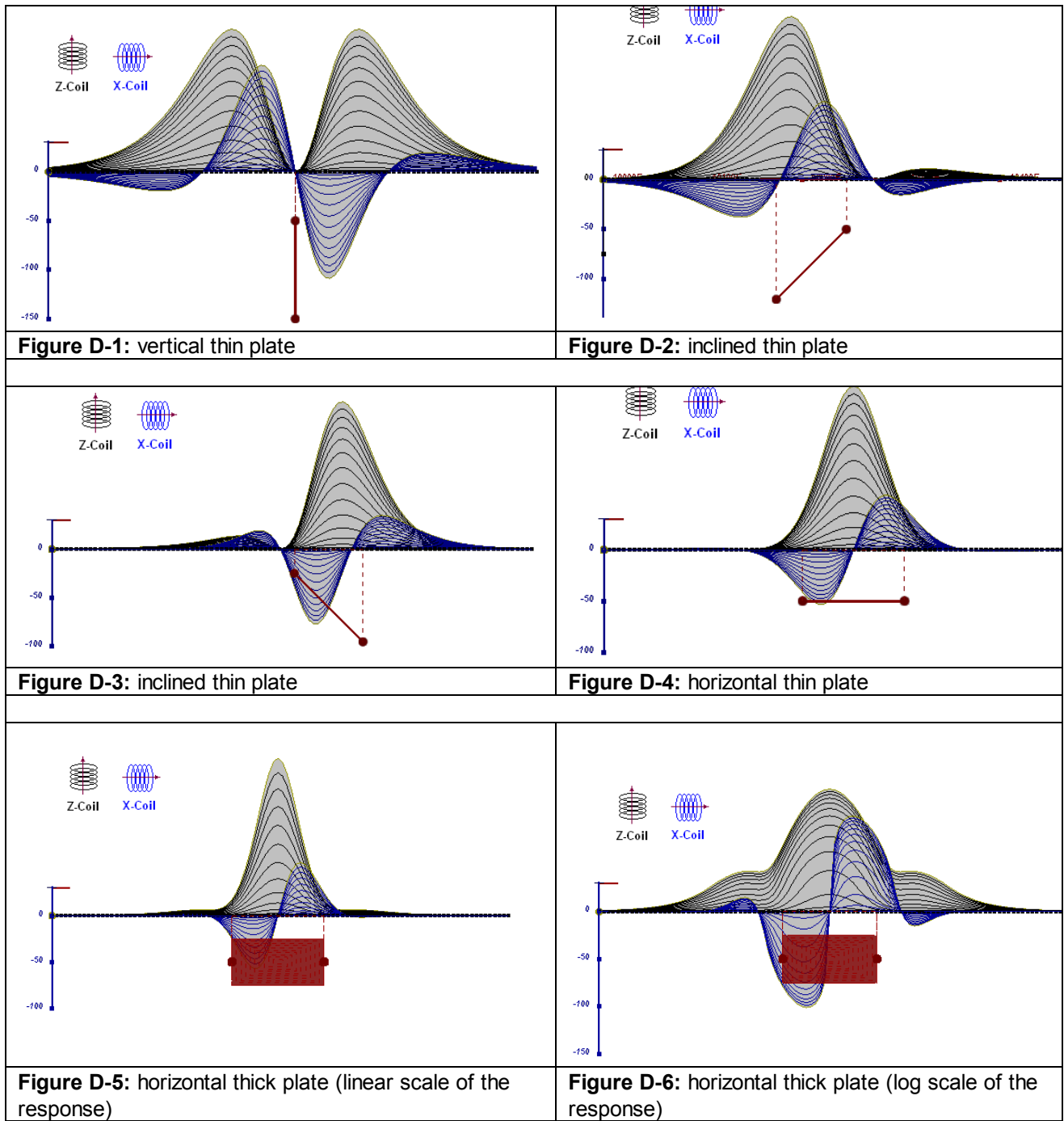
During turn-on and turn-off, a time varying field is produced (dB/dt) and an electro-motive force (emf) is created as a finite impulse response. A current ring around the transmitter loop moves outward and downward as time progresses. When conductive rocks and mineralization are encountered, a secondary field is created by mutual induction and measured by the receiver at the centre of the transmitter loop.

Efficient modeling of the results can be carried out on regularly shaped geometries, thus yielding close approximations to the parameters of the measured targets. The following is a description of a series of common models made for the purpose of promoting a general understanding of the measured results.

A set of models has been produced for the Geotech VTEM® system dB/dT Z and X components (see models D1 to D15). The Maxwell™ modeling program (EMIT Technology Pty. Ltd. Midland, WA, AU) used to generate the following responses assumes a resistive half-space. The reader is encouraged to review these models, so as to get a general understanding of the responses as they apply to survey results. While these models do not begin to cover all possibilities, they give a general perspective on the simple and most commonly encountered anomalies.

As the plate dips and departs from the vertical position, the peaks become asymmetrical.

As the dip increases, the aspect ratio (Min/Max) decreases and this aspect ratio can be used as an empirical guide to dip angles from near 90° to about 30°. The method is not sensitive enough where dips are less than about 30°.



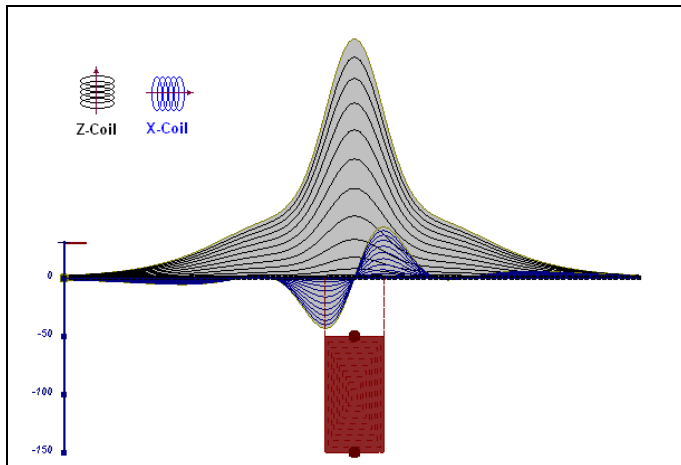


Figure D-7: vertical thick plate (linear scale of the response). 50 m depth

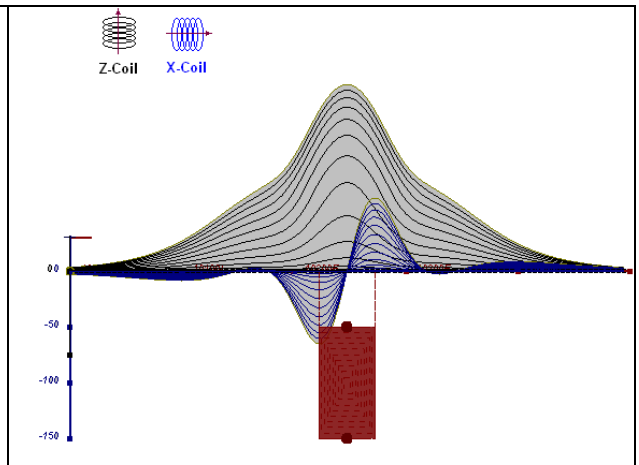


Figure D-8: vertical thick plate (log scale of the response). 50 m depth

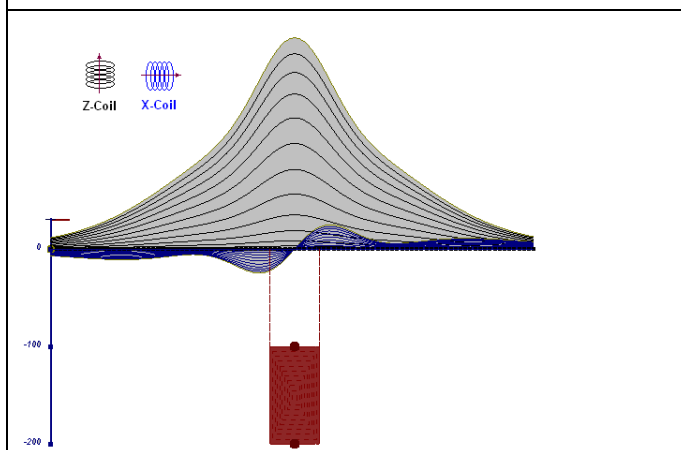


Figure D-9: vertical thick plate (linear scale of the response). 100 m depth

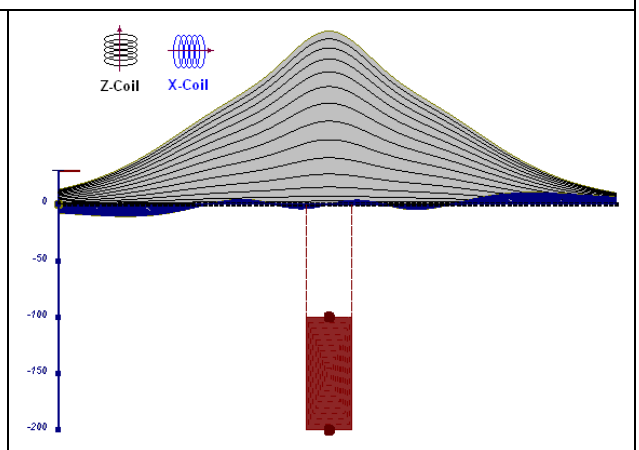


Figure D-10: vertical thick plate (linear scale of the response). Depth/hor.thickness=2.5

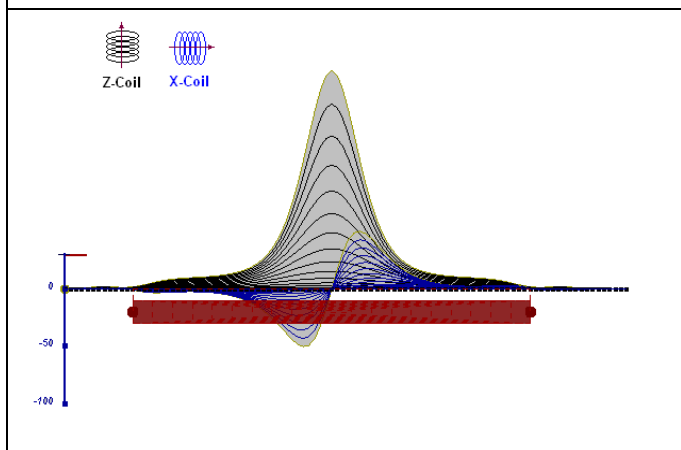


Figure D-10: horizontal thick plate (linear scale of the response)

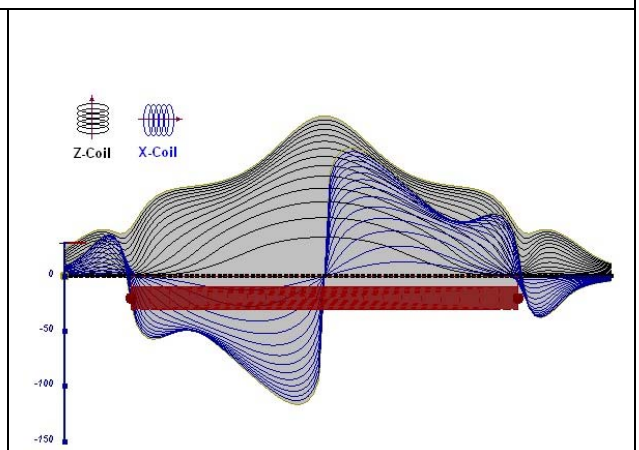


Figure D-11: horizontal thick plate (log scale of the response)

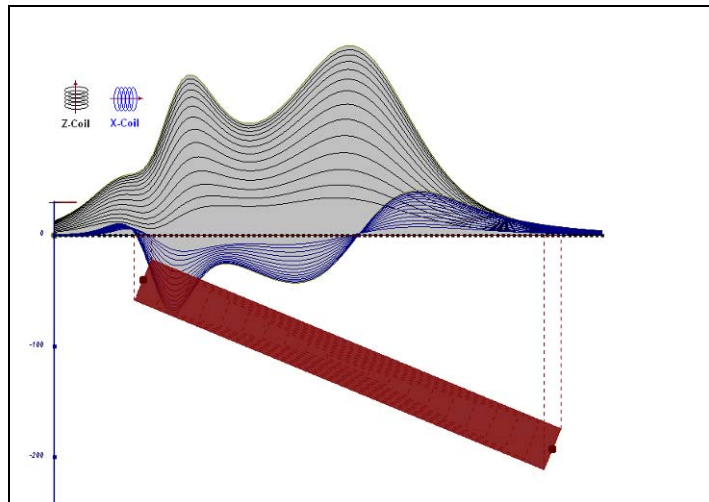


Figure D-12: inclined long thick plate

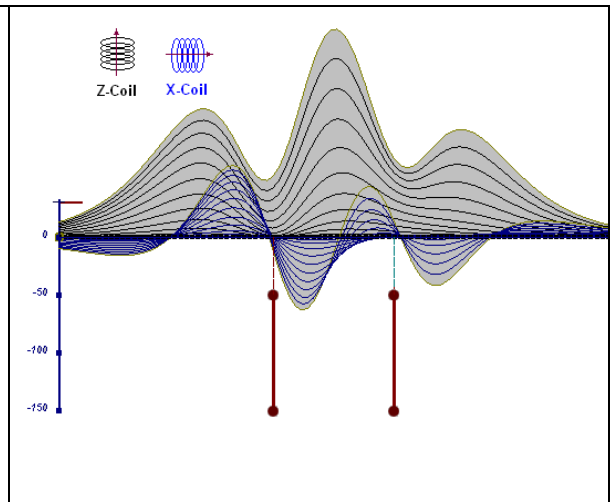


Figure D-13: two vertical thin plates

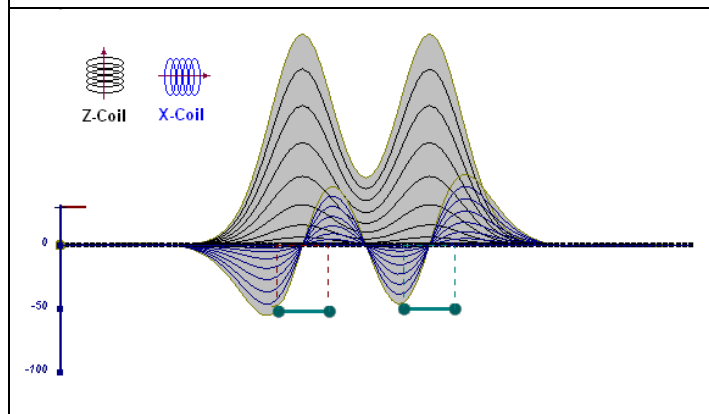


Figure D-14: two horizontal thin plates

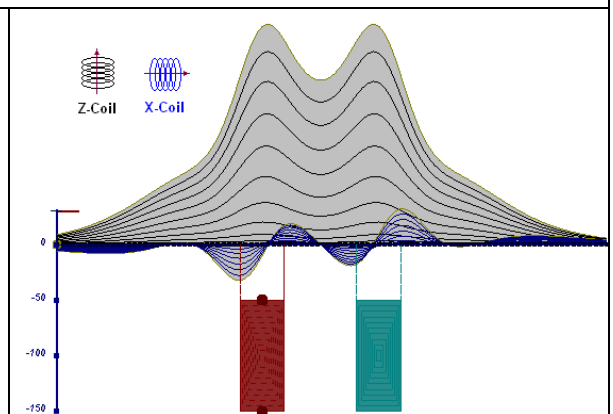


Figure D-15: two vertical thick plates

The same type of target but with different thickness, for example, creates different form of the response:

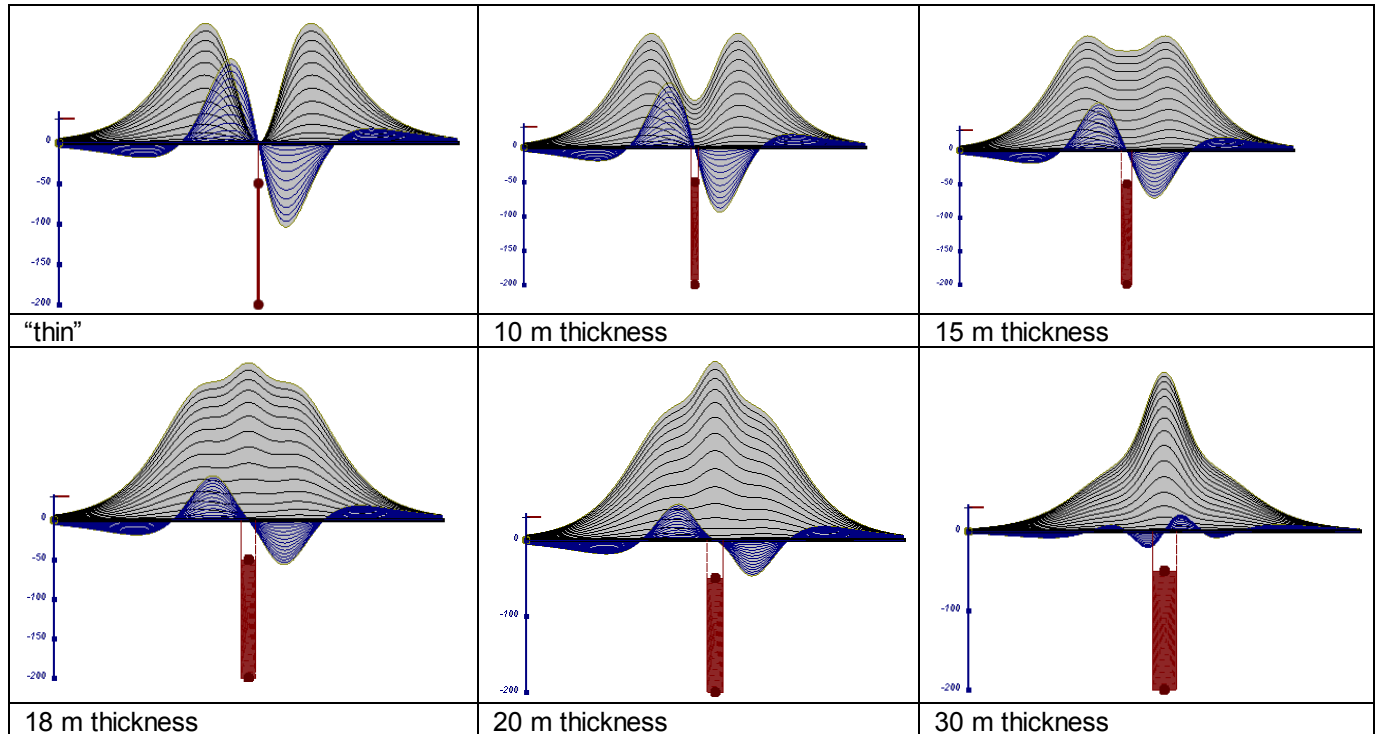


Figure D-16: Conductive vertical plate, depth 50 m, strike length 200 m, depth extend 150 m.

Alexander Prikhodko, PhD, P.Geo
Geotech Ltd.

September 2010

APPENDIX E

EM TIME CONSTANT (TAU) ANALYSIS

Estimation of time constant parameter¹ in transient electromagnetic method is one of the steps toward the extraction of the information about conductances beneath the surface from TEM measurements.

The most reliable method to discriminate or rank conductors from overburden, background or one and other is by calculating the EM field decay time constant (TAU parameter), which directly depends on conductance despite their depth and accordingly amplitude of the response.

Theory

As established in electromagnetic theory, the magnitude of the electro-motive force (emf) induced is proportional to the time rate of change of primary magnetic field at the conductor. This emf causes eddy currents to flow in the conductor with a characteristic transient decay, whose Time Constant (Tau) is a function of the conductance of the survey target or conductivity and geometry (including dimensions) of the target. The decaying currents generate a proportional secondary magnetic field, the time rate of change of which is measured by the receiver coil as induced voltage during the Off time.

The receiver coil output voltage (e_0) is proportional to the time rate of change of the secondary magnetic field and has the form,

$$e_0 \propto (1 / \tau) e^{-(t / \tau)}$$

Where,

$\tau = L/R$ is the characteristic time constant of the target (TAU)

R = resistance

L = inductance

From the expression, conductive targets that have small value of resistance and hence large value of τ yield signals with small initial amplitude that decays relatively slowly with progress of time. Conversely, signals from poorly conducting targets that have large resistance value and small τ , have high initial amplitude but decay rapidly with time¹ (Figure E-1).

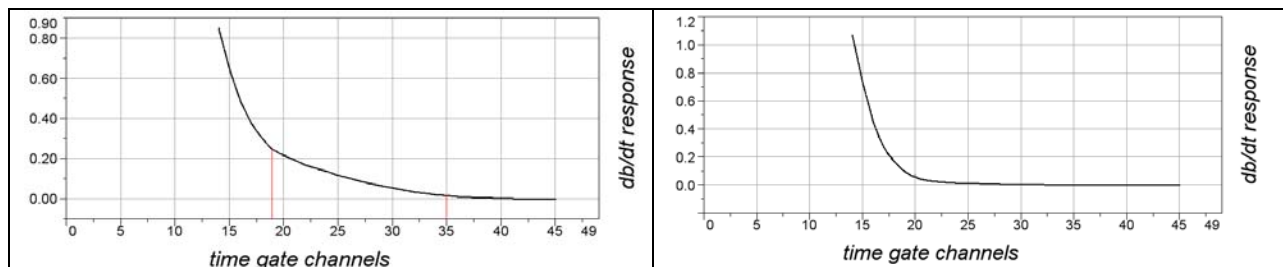


Figure E-1: Left – presence of good conductor, right – poor conductor.

¹ McNeill, JD, 1980, "Applications of Transient Electromagnetic Techniques", Technical Note TN-7 page 5, Geonics Limited, Mississauga, Ontario.

EM Time Constant (Tau) Calculation

The EM Time-Constant (TAU) is a general measure of the speed of decay of the electromagnetic response and indicates the presence of eddy currents in conductive sources as well as reflecting the “conductance quality” of a source. Although TAU can be calculated using either the measured dB/dt decay or the calculated B-field decay, dB/dt is commonly preferred due to better stability (S/N) relating to signal noise. Generally, TAU calculated on base of early time response reflects both near surface overburden and poor conductors whereas, in the late ranges of time, deep and more conductive sources, respectively. For example early time TAU distribution in an area that indicates conductive overburden is shown in Figure 2.

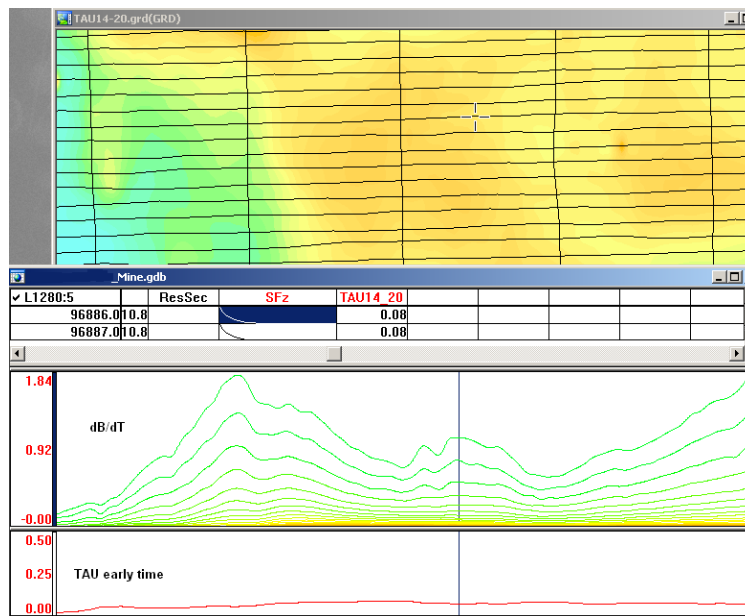


Figure E-2: Map of early time TAU Area with overburden conductive layer and local sources.

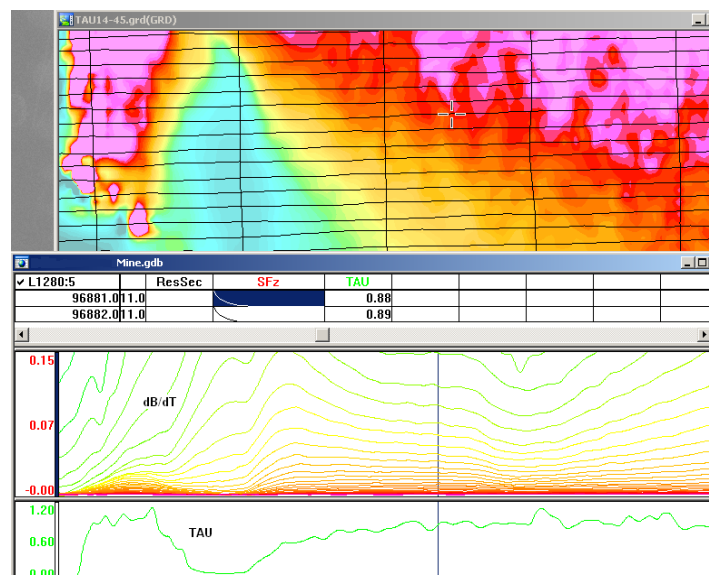


Figure E-3: Map of full time range TAU with EM anomaly due to deep highly conductive target.

There are many advantages of TAU maps:

- TAU depends only on one parameter (conductance) in contrast to response magnitude;
- TAU is integral parameter, which covers time range and all conductive zones and targets are displayed independently of their depth and conductivity on a single map.
- Very good differential resolution in complex conductive places with many sources with different conductivity.
- Signs of the presence of good conductive targets are amplified and emphasized independently of their depth and level of response accordingly.

In the example shown in Figure 4 and 5, three local targets are defined, each of them with a different depth of burial, as indicated on the resistivity depth image (RDI). All are very good conductors but the deeper target (number 2) has a relatively weak dB/dt signal yet also features the strongest total TAU (Figure 4). This example highlights the benefit of TAU analysis in terms of an additional target discrimination tool.

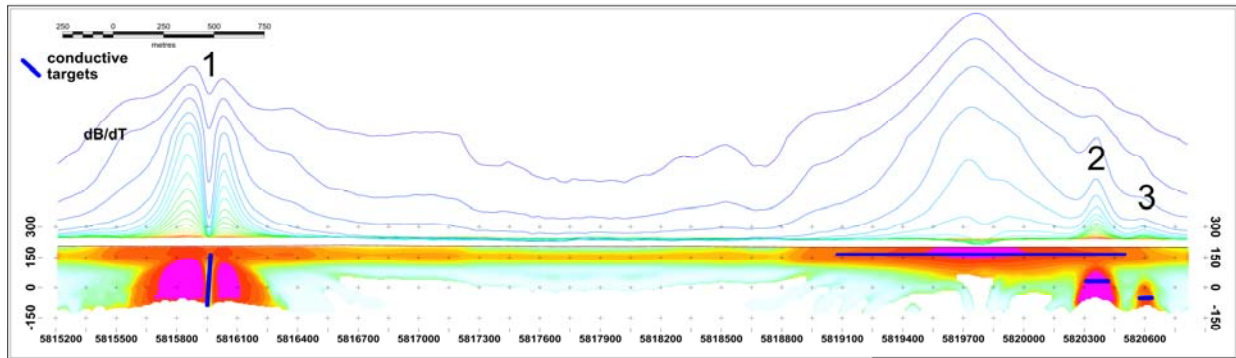


Figure E-4: dB/dt profile and RDI with different depths of targets.

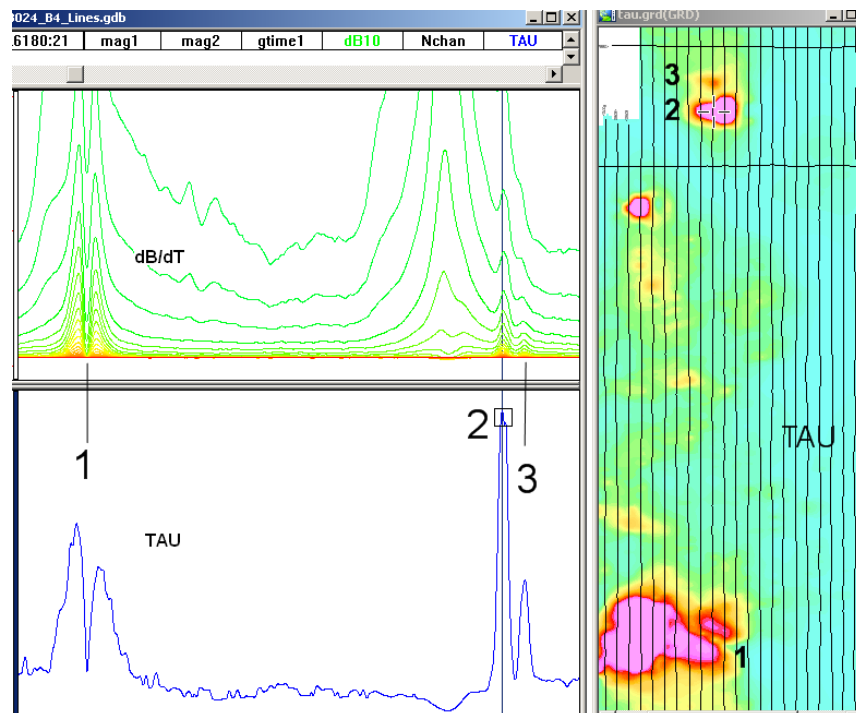


Figure E-5: Map of total TAU and dB/dt profile.

The EM Time Constants for dB/dt and B-field were calculated using the “sliding Tau” in-house program developed at Geotech2. The principle of the calculation is based on using of time window (4 time channels) which is sliding along the curve decay and looking for latest time channels which have a response above the level of noise and decay. The EM decays are obtained from all available decay channels, starting at the latest channel. Time constants are taken from a least square fit of a straight-line (log/linear space) over the last 4 gates above a pre-set signal threshold level (Figure E-6). Threshold settings are pointed in the “label” property of TAU database channels. The sliding Tau method determines that, as the amplitudes increase, the time-constant is taken at progressively later times in the EM decay. Conversely, as the amplitudes decrease, Tau is taken at progressively earlier times in the decay. If the maximum signal amplitude falls below the threshold, or becomes negative for any of the 4 time gates, then Tau is not calculated and is assigned a value of “dummy” by default.

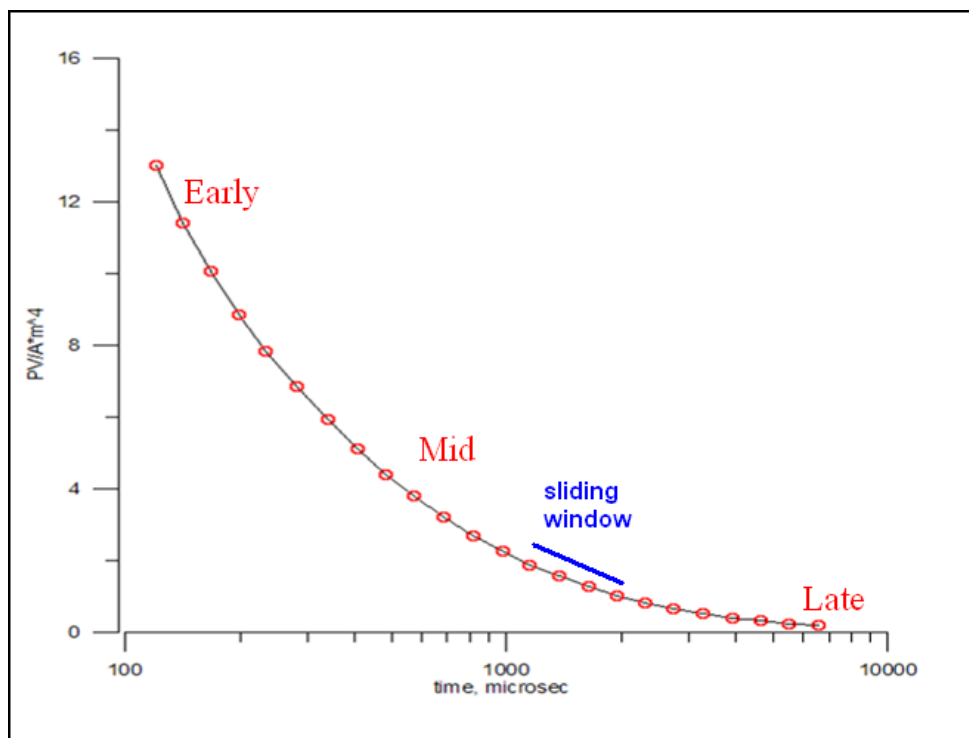


Figure E-6: Typical dB/dt decays of VTEM data

Alexander Prikhodko, PhD, P. Geo
Geotech Ltd.

September 2010

² by A.Prikhodko

APPENDIX F

TEM RESISTIVITY DEPTH IMAGING (RDI)

Resistivity depth imaging (RDI) is a technique used to rapidly convert EM profile decay data into an equivalent resistivity versus depth cross-section, by deconvolving the measured TEM data. The used RDI algorithm of Resistivity-Depth transformation is based on the scheme of the apparent resistivity transform of Maxwell A. Meju (1998)¹ and TEM response from a conductive half-space. The program is developed by Alexander Prikhodko and is depth calibrated based on forward plate modeling for a VTEM system configuration (Fig. 1-10).

RDI provides reasonable indications of conductor relative depth and vertical extent, as well as an accurate 1D layered-earth apparent conductivity/resistivity structure across VTEM flight lines. Approximate depth of investigation of a TEM system, image of secondary field distribution in half-space, effective resistivity, initial geometry and position of conductive targets is the information obtained on the basis of the RDI.

Maxwell forward modeling with RDI sections from the synthetic responses (VTEM system)

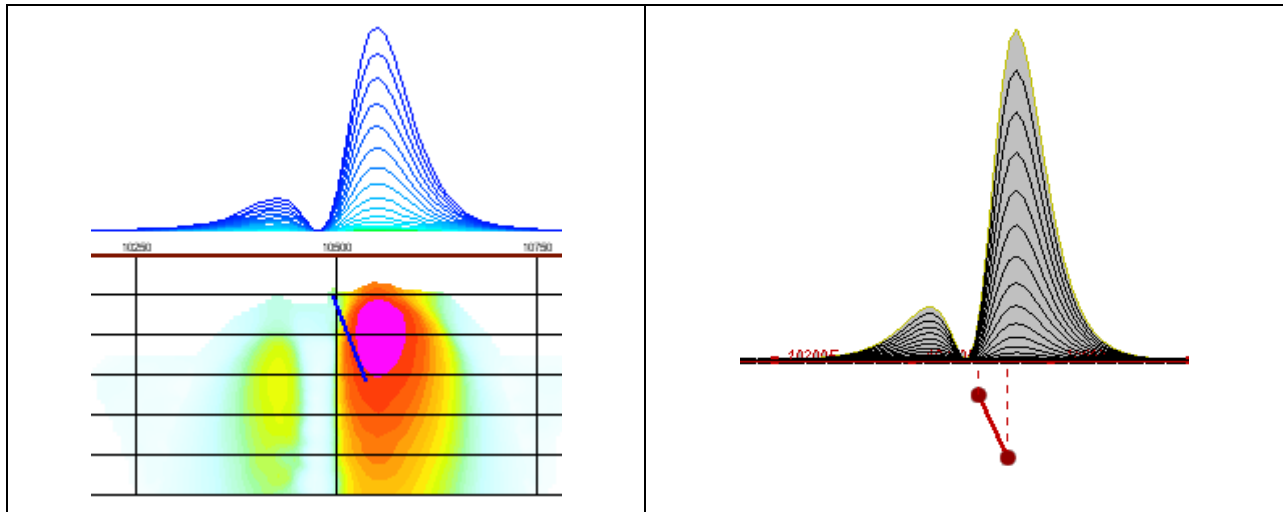


Figure F-1: Maxwell plate model and RDI from the calculated response for a conductive “thin” plate (depth 50 m, dip 65 degree, depth extend 100 m).

¹ Maxwell A. Meju, 1998, Short Note: A simple method of transient electromagnetic data analysis, *Geophysics*, **63**, 405–410.

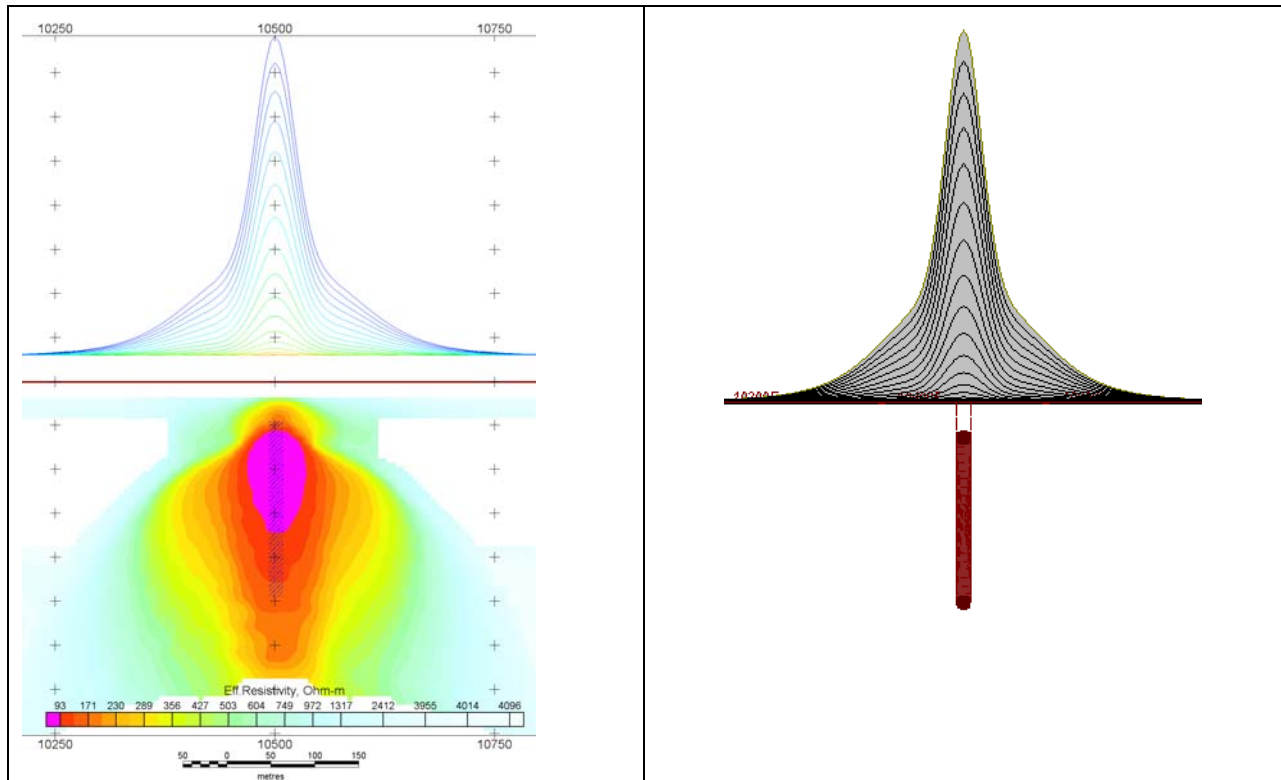


Figure F-2: Maxwell plate model and RDI from the calculated response for “thick” plate 18 m thickness, depth 50 m, depth extend 200 m).

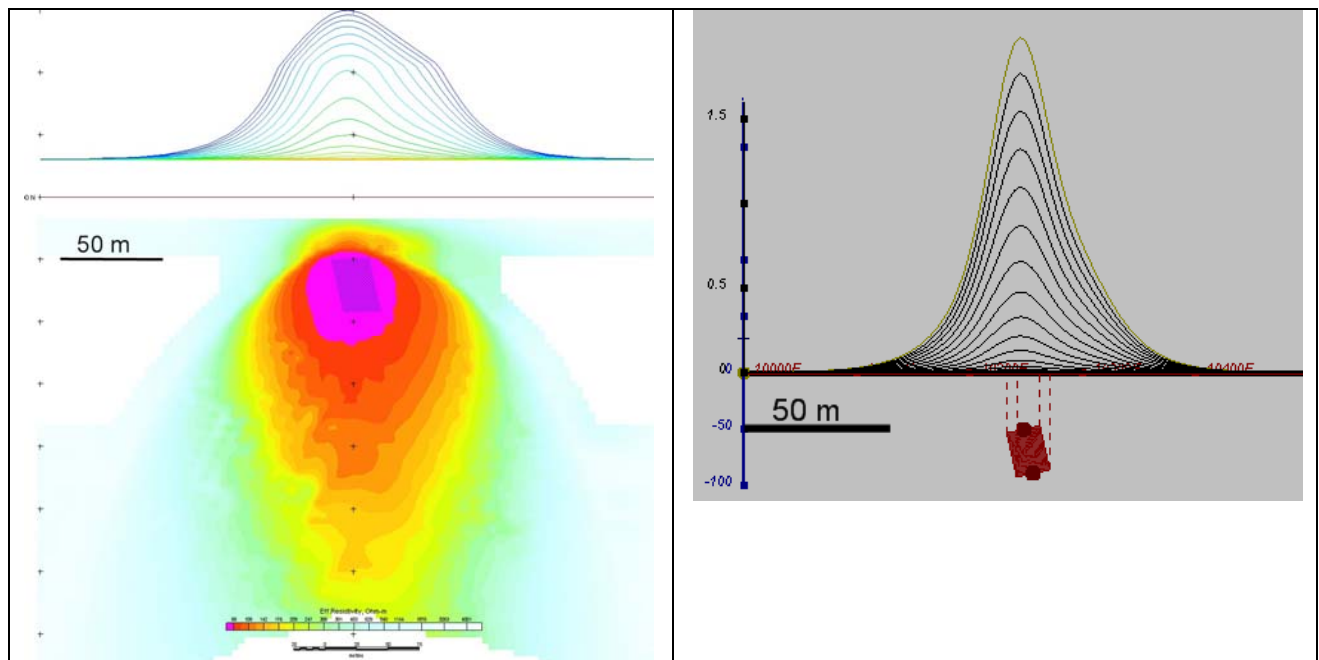


Figure F-3: Maxwell plate model and RDI from the calculated response for bulk (“thick”) 100 m length, 40 m depth extend, 30 m thickness

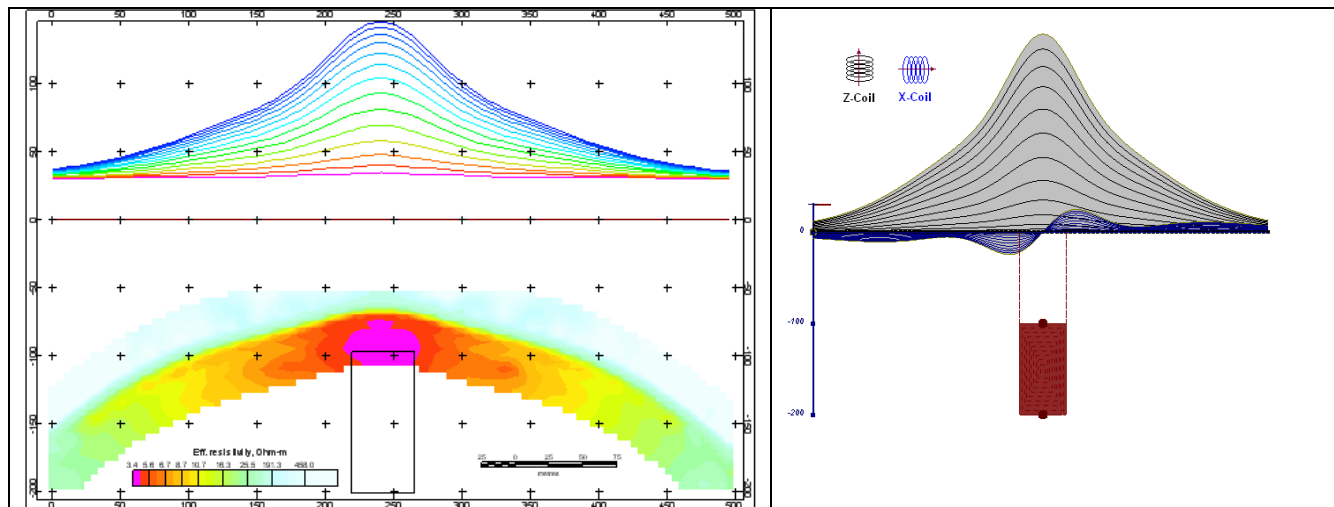


Figure F-4: Maxwell plate model and RDI from the calculated response for “thick” vertical target (depth 100 m, depth extend 100 m). 19-44 chan.

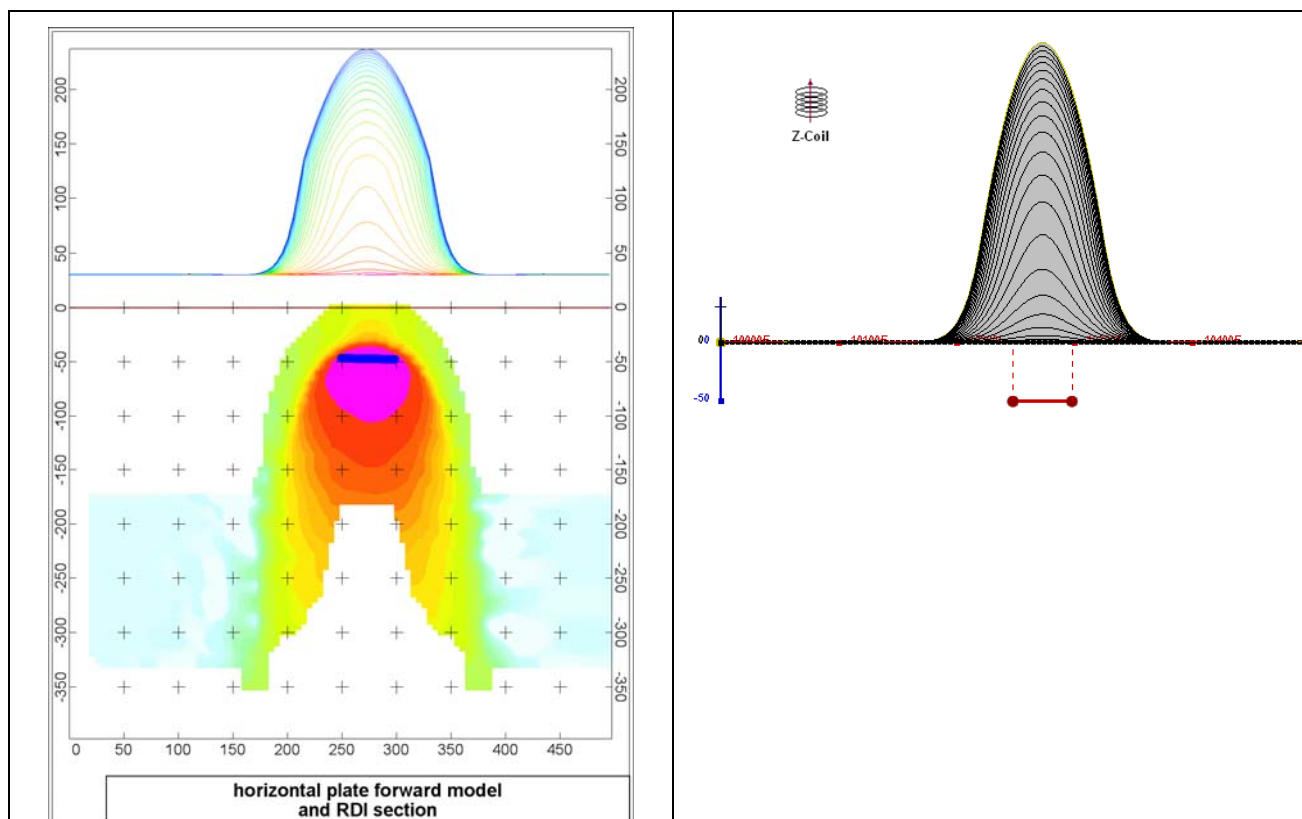


Figure F-5: Maxwell plate model and RDI from the calculated response for horizontal thin plate (depth 50 m, dim 50x100 m). 15-44 chan.

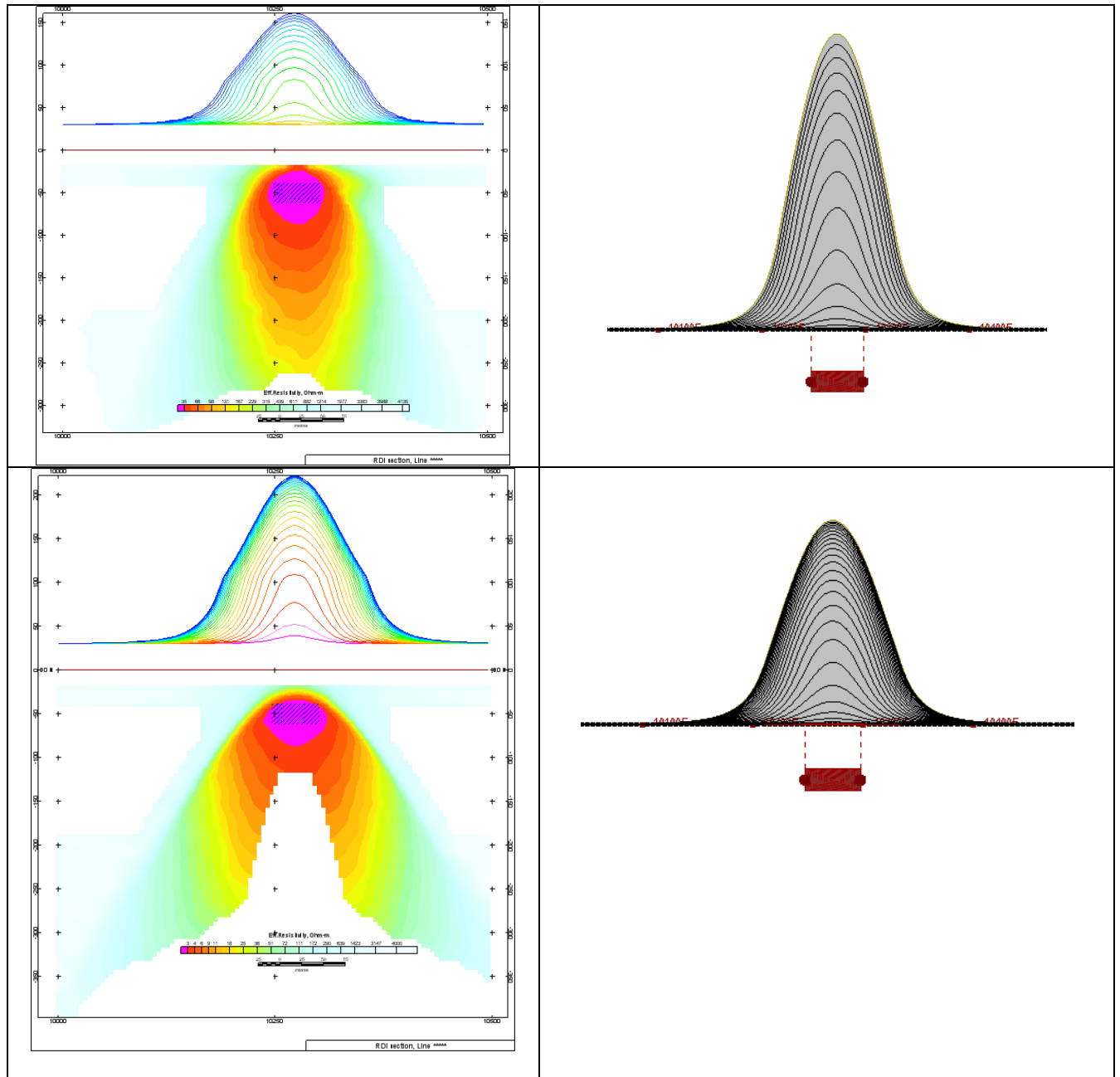


Figure F-6: Maxwell plate model and RDI from the calculated response for horizontal thick (20m) plate – less conductive (on the top), more conductive (below)

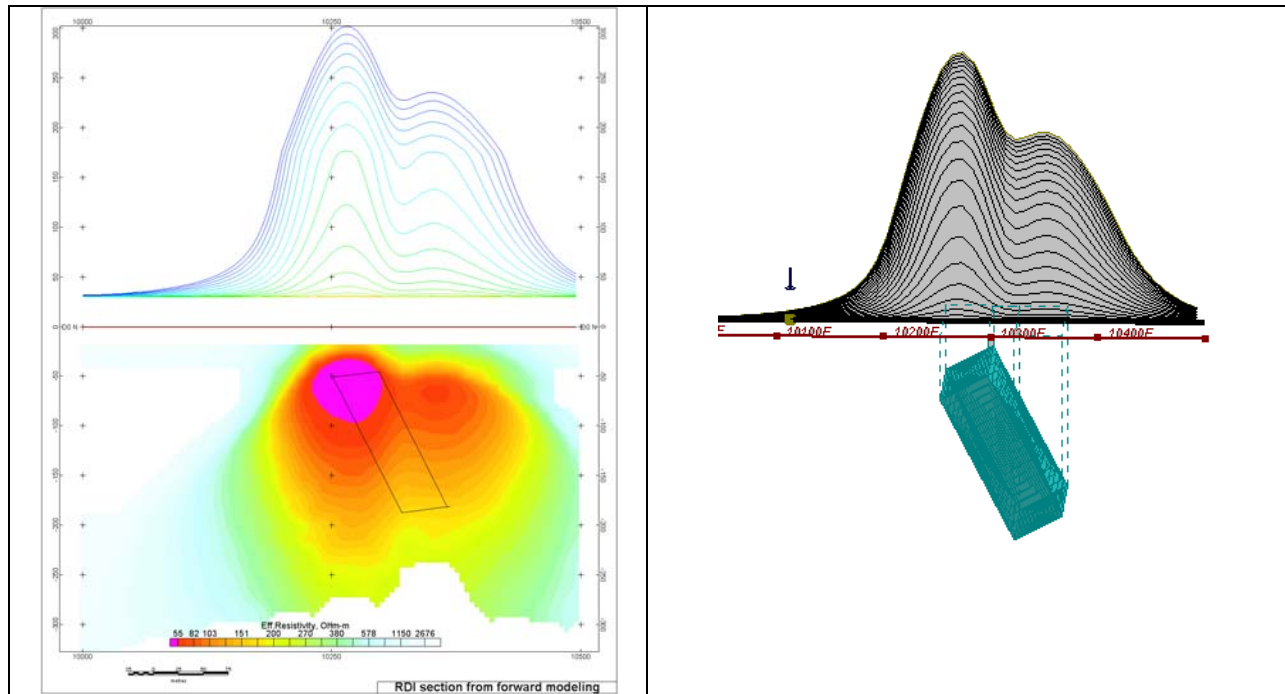


Figure G-7: Maxwell plate model and RDI from the calculated response for inclined thick (50m) plate. Depth extends 150 m, depth to the target 50 m.

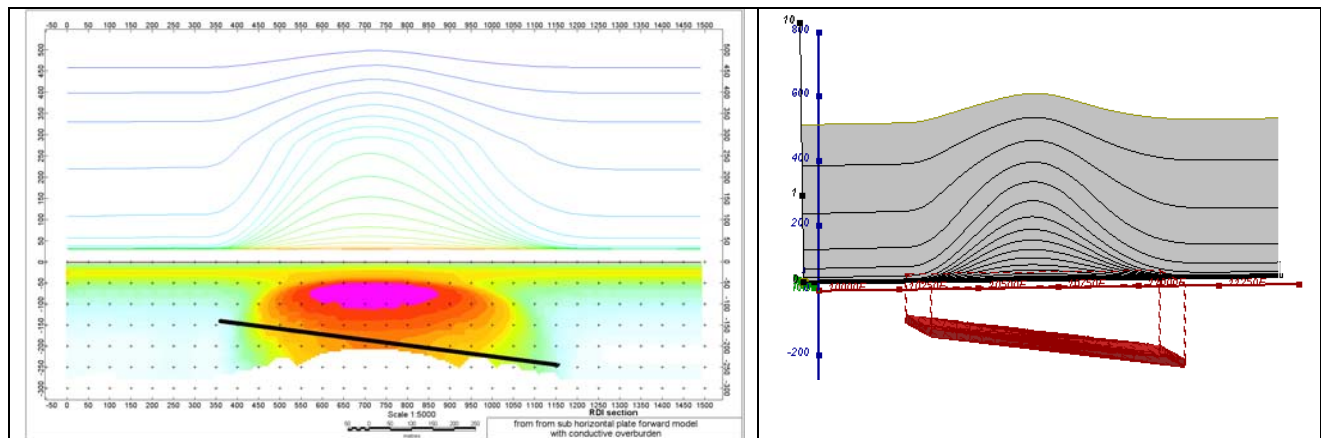


Figure F-8: Maxwell plate model and RDI from the calculated response for the long, wide and deep subhorizontal plate (depth 140 m, dim 25x500x800 m) with conductive overburden.

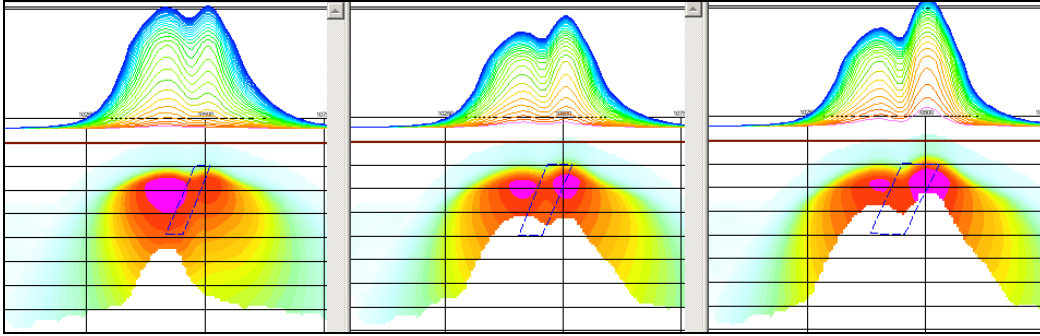


Figure F-9: Maxwell plate models and RDIs from the calculated response for “thick” dipping plates (35, 50, 75 m thickness), depth 50 m, conductivity 2.5 S/m.

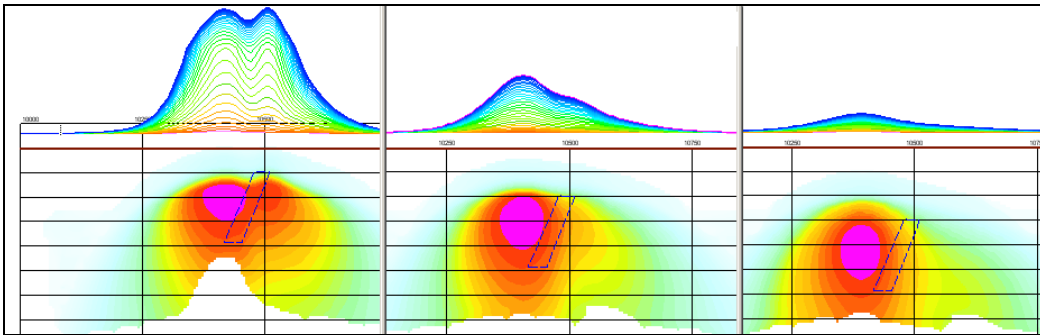


Figure F-10: Maxwell plate models and RDIs from the calculated response for “thick” (35 m thickness) dipping plate on different depth (50, 100, 150 m), conductivity 2.5 S/m.

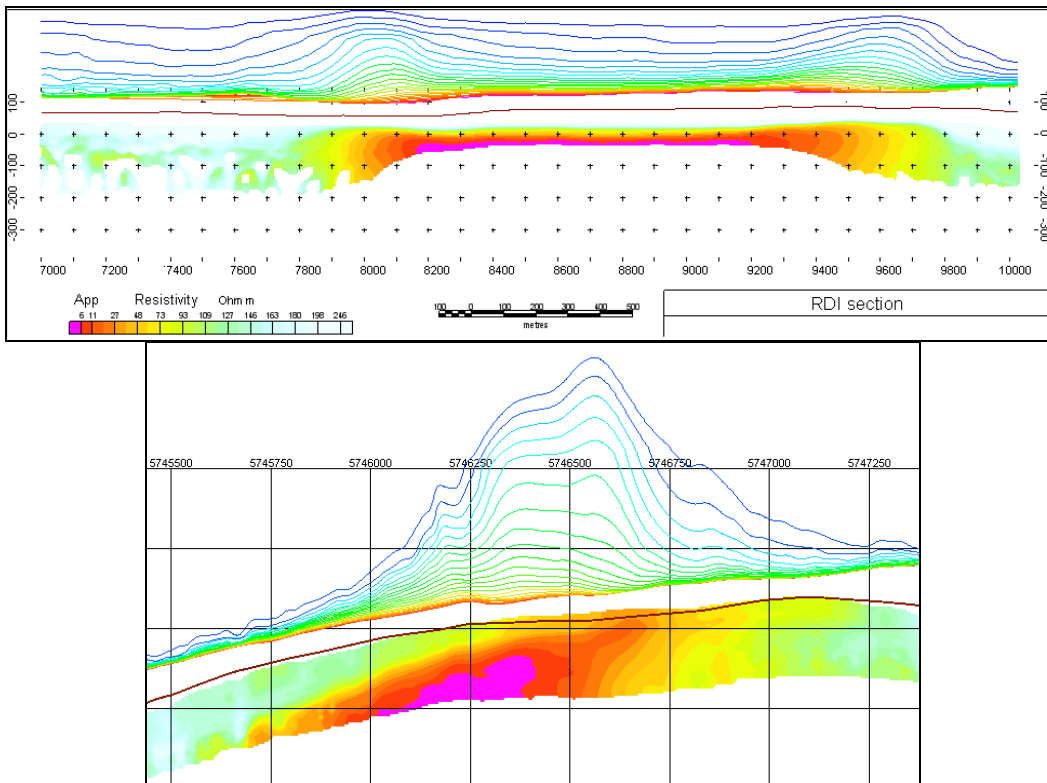
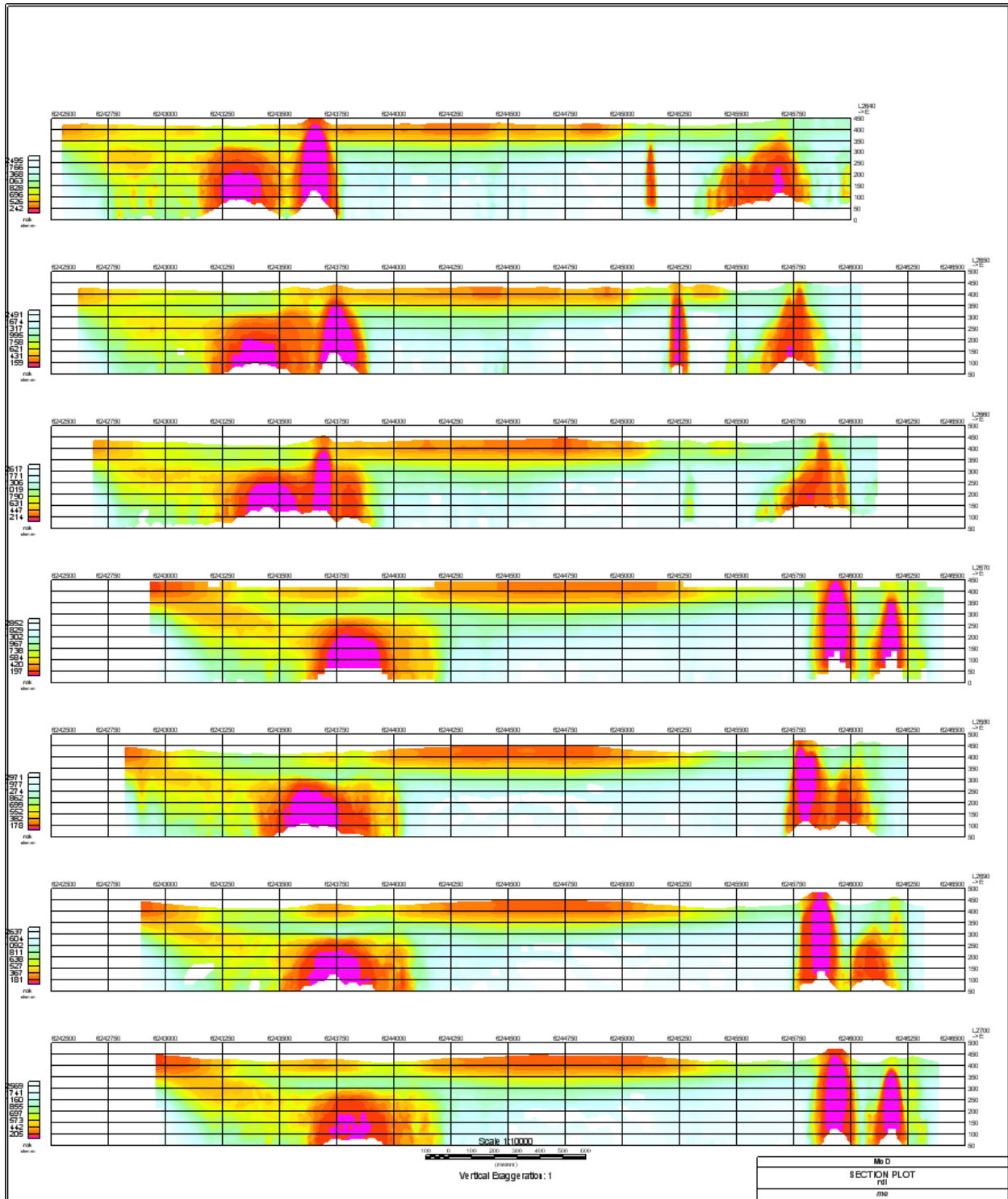


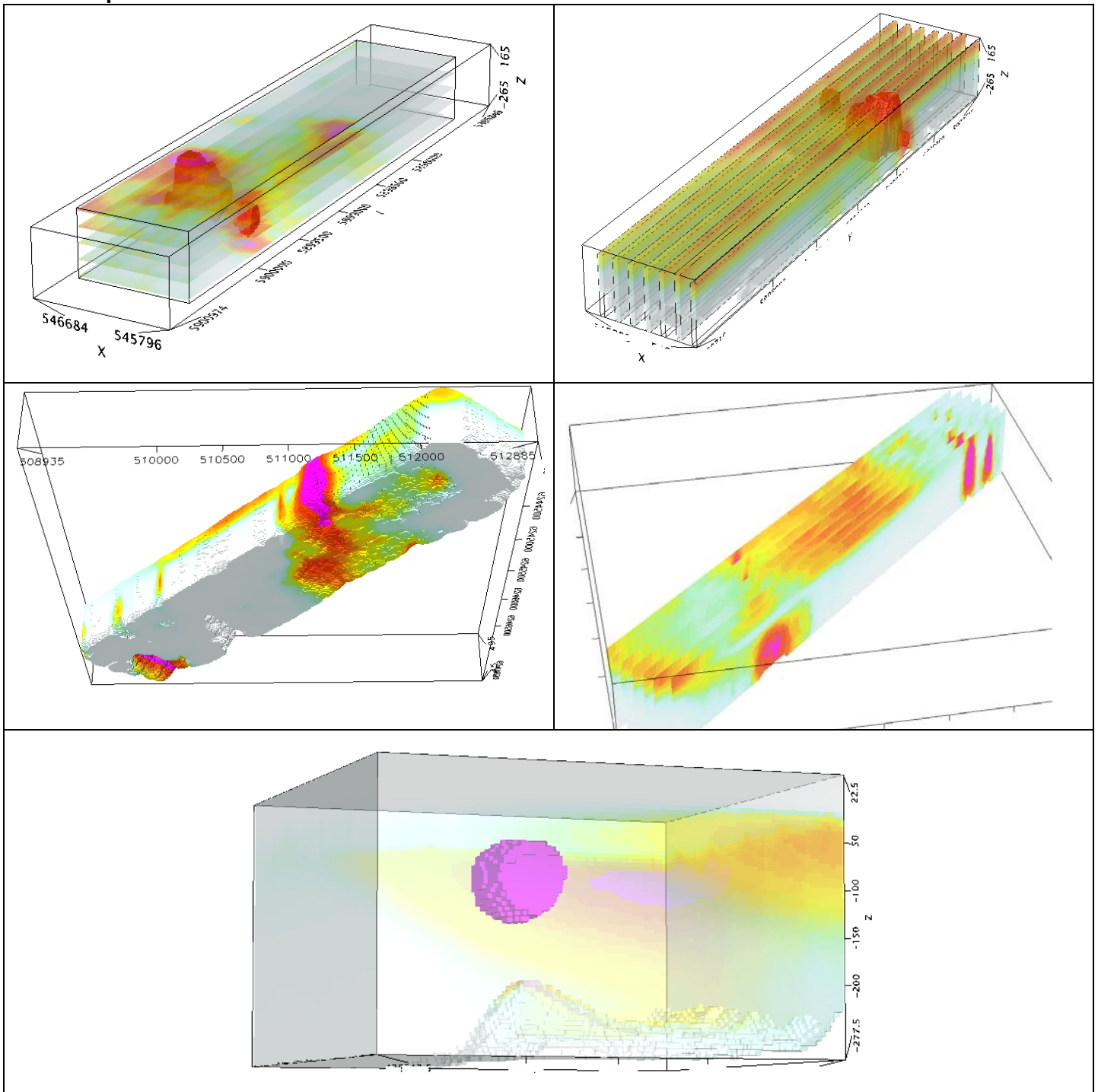
Figure F-11: RDI section for the real horizontal and slightly dipping conductive layers

FORMS OF RDI PRESENTATION

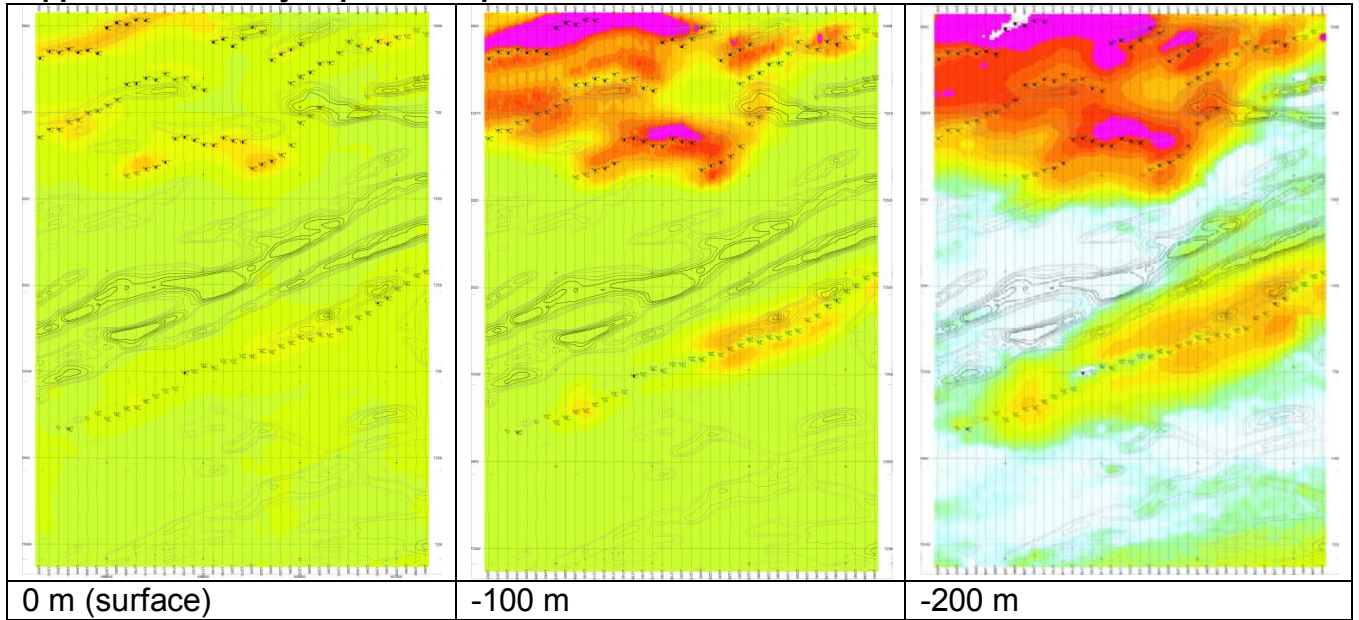
Presentation of series of lines



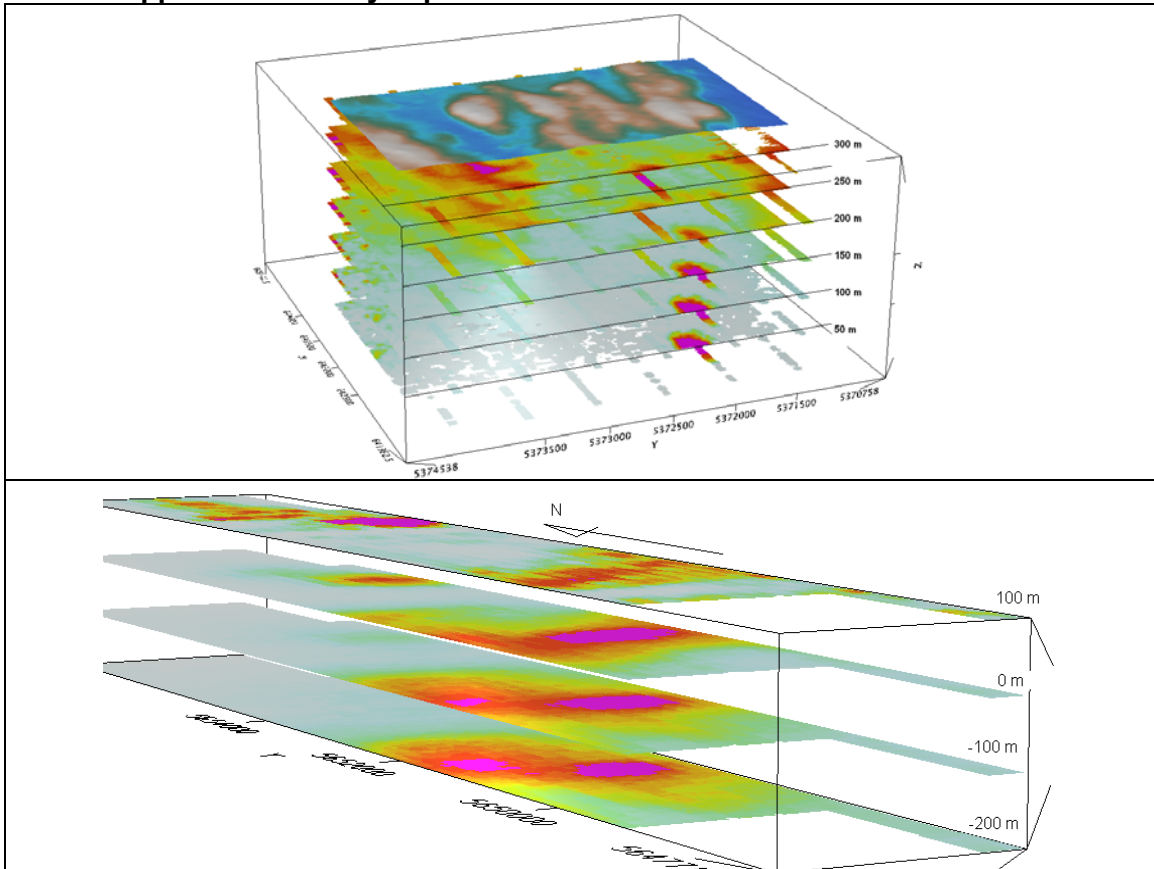
3d presentation of RDIs



Apparent Resistivity Depth Slices plans:

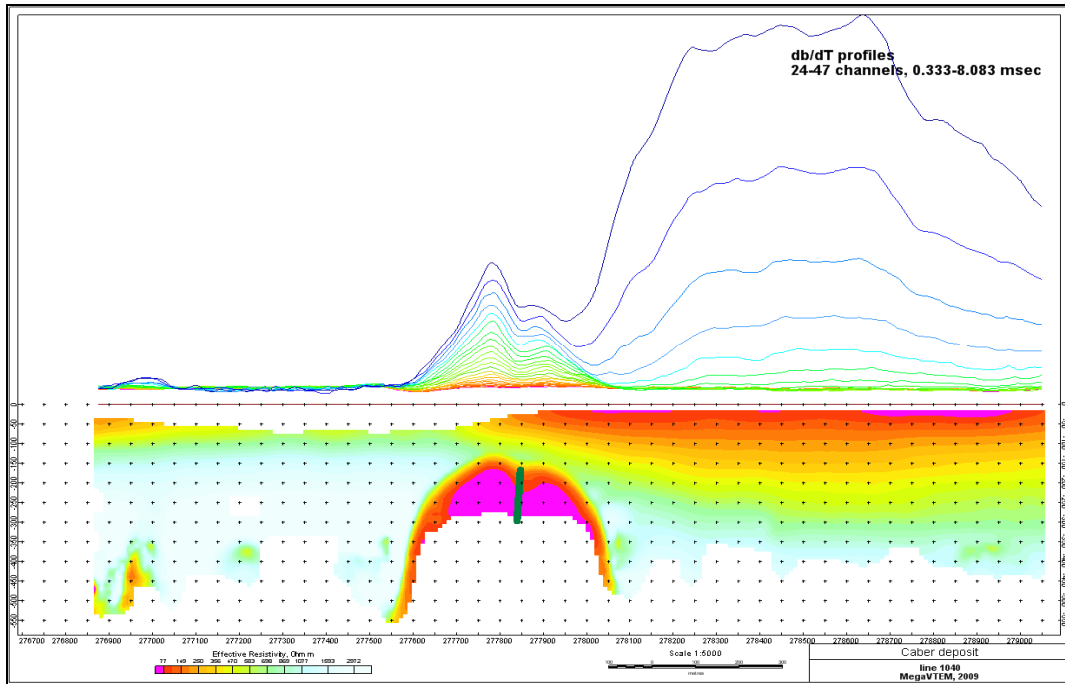


3d views of apparent resistivity depth slices:

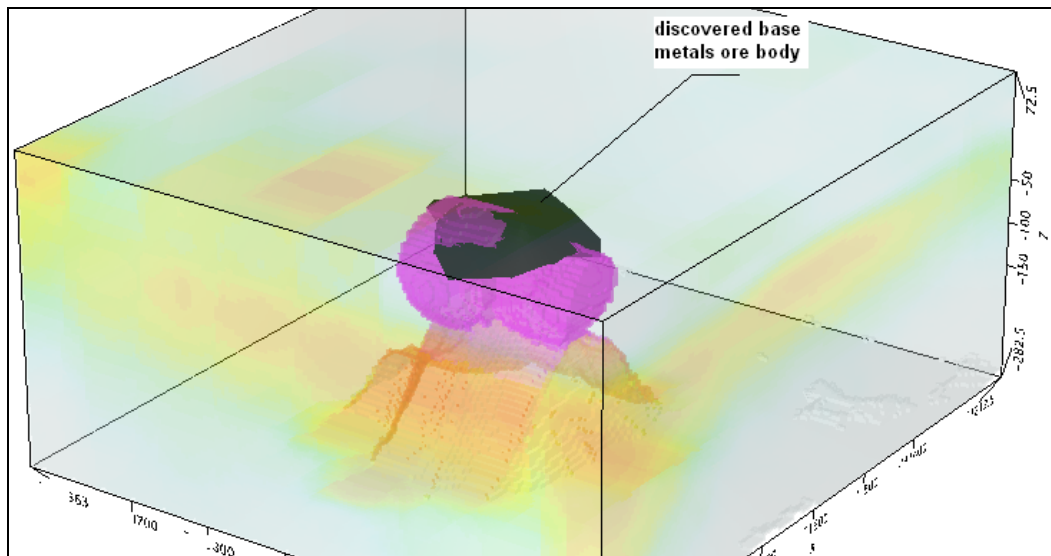


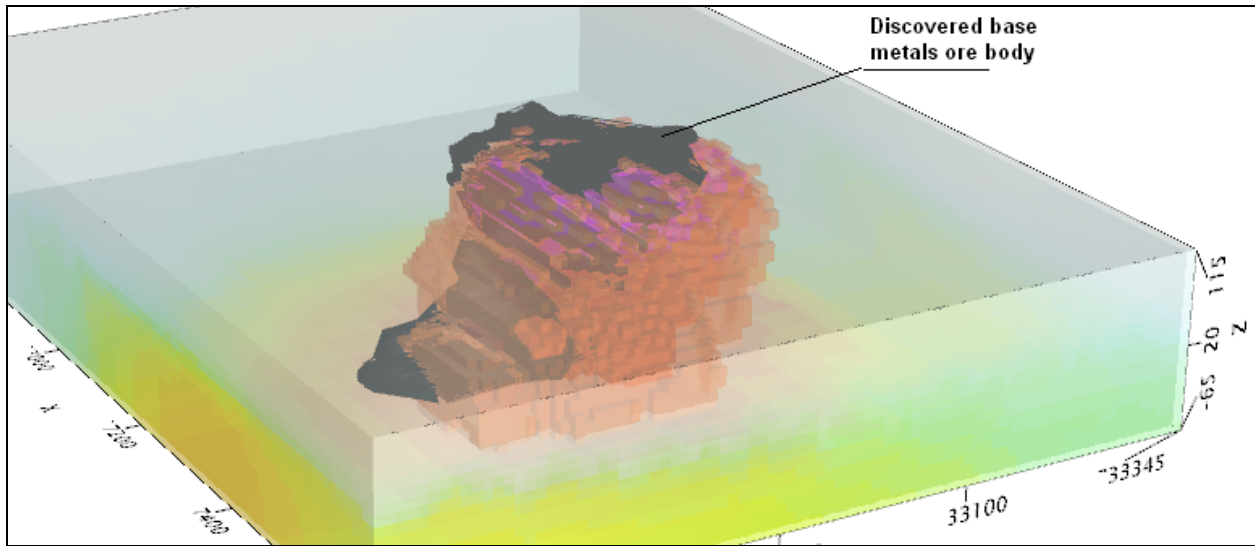
Real base metal targets in comparison with RDIs:

RDI section of the line over Caber deposit (“thin” subvertical plate target and conductive overburden).



3d RDI voxels with base metals ore bodies (Middle East):





Alexander Prihodko, PhD, P.Geo
Geotech Ltd.
April 2011

APPENDIX G

Resistivity Depth Images (RDI)

Please see DVD RDI folder for PDFs GL140269_RDIs_Expo and GL140269_RDIs_Ellen